Quantifying Seasonal Seagrass Effects on Flow and Sediment Dynamics in a Back-barrier Bay

Qingguang Zhu[1], Patricia L. Wiberg[1], Matthew A. Reidenbach[1]

[1]Department of Environmental Sciences, University of Virginia, Charlottesville, VA, USA

Corresponding author: Qingguang Zhu (qz3cp@virginia.edu)

Key Points:

- A coupled flow-wave-vegetation-sediment interaction model was used to investigate spatial and seasonal seagrass impacts in a coastal bay
- Large reductions in sediment resuspension in dense meadows were mainly caused by flow retardation rather than wave attenuation
- Small changes in winter seagrass density resulted in strong changes in net sediment flux into/out of the meadow

This article has been accepted for publication and undergone full peer review but has not been through the copyediting, typesetting, pagination and proofreading process, which may lead to differences between this version and the Version of Record. Please cite this article as doi: 10.1029/2020JC016547.

Abstract

Seagrass growth and senescence exert a strong influence on flow structure and sediment transport processes in coastal environments. However, most previous studies of seasonal seagrass effects either focused on small-scale field measurements or did not fully resolve the synergistic effects of flow-wave-vegetation-sediment interaction at a meadow scale. In this study, we applied a coupled Delft3D-FLOW and SWAN model that included effects of seagrass on flow, waves, and sediment resuspension in a shallow coastal bay to quantify seasonal seagrass impacts on bay dynamics. The model was extensively validated using seasonal field hydrodynamic and suspended sediment data within a seagrass meadow and a nearby unvegetated site. Our results show that seagrass meadows significantly attenuated flow (60%) and waves (20%) and reduced suspended sediment concentration (85%) during summer when its density reached a maximum. Probability density distributions of combined wave-current bed shear stress within the seagrass meadow indicate that significant reductions in sediment resuspension during summer were mainly caused by flow retardation rather than wave attenuation. Although low-density seagrass in winter resulted in much smaller reductions in flow and waves compared with summer meadows, small changes in winter seagrass density resulted in large differences in the magnitude of attenuation of flow and shear stress. Similarly, while high seagrass densities effectively trapped sediment during summer, small changes in winter density resulted in strong changes in net sediment flux into/out of the meadow. At our study site, low seagrass densities provided significant reductions in wintertime sediment loss compared to losses associated with completely unvegetated conditions.

Plain Language Summary

Seagrasses are valuable ecosystems that inhabit shallow coastal waters. In summertime, their dense canopies can significantly slow tidal currents and lower wave energy, thereby reducing sediment resuspension and improving light environments for seagrass growth. This strong seagrass control on bay dynamics diminishes during winter, however, when seagrass density is low. In order to better understand seasonal seagrass impacts on shallow coastal environments, we ran a coastal model that includes effects of seagrass on flow, waves, and sediment resuspension under both summer and winter conditions in a shallow coastal bay. We found that dense seagrass during summer can considerably lower the energy levels of the bay and effectively trap fine particles. The strong reductions in sediment resuspension are mainly due to flow reduction caused by seagrass rather than wave attenuation. During winter, although low densities of seagrass had relatively limited effects on flow and waves, vegetation was still very important to protect the seabed from erosion. Our model predicts a small change of seagrass density in winter could result in strong changes in sediment input/output of the meadows. This effect had not been well characterized before, and it is important to understand because it has a significant impact on seagrass ecosystems.

1 Introduction

Seagrasses are important ecosystems that inhabit shallow coastal waters. They offer valuable ecosystem services (e.g., nutrient cycling, water quality control, and carbon sequestration) and provide favorable habitat for species (McGlathery et al., 2007; Nagelkerken et al., 2000; Oreska et al., 2017). They are also commonly referred to as natural eco-engineers that can effectively modify physical environments and stabilize the seabed (Jones et al., 1994). Previous studies on seagrass interactions with physical environments have shown that seagrasses

can significantly modify the mean flow and turbulent structure (Fonseca & Fisher, 1986; Gambi et al., 1990; Hansen & Reidenbach, 2012; Koch & Gust, 1999; Widdows et al., 2008); and efficiently dissipate wave energy and attenuate wave height (Fonseca & Cahalan, 1992; Paul et al., 2012; Reidenbach & Thomas, 2018). Attenuation of currents and waves promotes suspended sediment deposition and increases water column clarity (Carr et al., 2010; De Boer, 2007; Gacia et al., 2003).

Despite their great importance in coastal ecosystems, seagrasses are one of the most rapidly declining marine habitats, threatened by eutrophication, temperature stress, and anthropogenic stressors (Orth et al., 2006; Waycott et al., 2009). Understanding state change dynamics and the response of seagrass ecosystems to climate change and human disturbance requires greater insights into flow-wave-vegetation-sediment interactions (McGlathery et al., 2013). Previous studies of seagrass effects on flow and sediment dynamics have mainly focused on laboratory investigations and small-scale and short-term field measurements, and have addressed many key questions in vegetated flow dynamics (e.g., De Boer, 2007; Ganthy et al., 2015; Hansen & Reidenbach, 2012; Nepf, 2012). However, these approaches cannot resolve the inherent complexity and spatial variability of natural environments, including temporal and spatial variability of waves and currents, seabed sediment distribution and availability, spatial variations of bathymetry, and spatial extent and density of subtidal and intertidal vegetation.

With the advancement of numerical model capability to include vegetation effects in flow and wave simulations, researchers have been able to better resolve the synergistic effects of flow-wave-vegetation-sediment interaction in spatially resolved settings. Chen et al. (2007) used a modified Nearshore Community model (NearCoM) that can account for seagrass effects on flow and waves to investigate the effects of seagrass on wave attenuation and suspended sediment transport, and predict the erosion and deposition pattern in an idealized seagrass bed in the nearshore ocean. Beudin et al. (2017) developed a coupled flow-wave-vegetation interaction model based on the Coupled-Ocean-Atmosphere-Wave-Sediment Transport (COAWST) modeling system to investigate the various interacting processes in an idealized shallow basin with a square seagrass patch (1 km by 1 km). Donatelli et al. (2018, 2019) applied this model in Barnegat Bay, USA, to quantify the effects of seagrass on hydrodynamics, wave energy, and sediment exchange between tidal flats covered by seagrass meadows and the adjacent salt marsh. Their results highlighted the complex dynamics between subtidal and intertidal landscapes and benefits of seagrass meadows in enhancing system resilience.

Although these coupled model simulations have significantly improved our understanding of seagrass impacts on flow and sediment dynamics, important aspects of seagrass-tidal flat systems still need to be investigated. Most studies do not provide direct validation with measured flow and suspended sediment data in seagrass meadows. Considering the inherent complexity of natural environments, model validation with spatially distributed data sets is necessary to obtain accurate flow patterns and sediment flux rates. Furthermore, seasonal seagrass growth and senescence in temperate climates exert a strong influence on reduction in flow and waves, and alter sediment resuspension and deposition on vegetated tidal flats (Gacia & Duarte, 2001; Ganthy et al., 2013; Hansen & Reidenbach, 2013; Hasegawa et al., 2008). Carr et al. (2018) found that low seagrass biomass in the fall/winter increased the amount of sediment resuspension in the bay, whereas dense seagrass during the growing season inhibited sediment resuspension and limited sediment delivery to adjacent salt marsh. These findings are based on long-term, transect-based simulations and do not resolve seasonal wind patterns or 2-D spatial

patterns of vegetation, flow, waves, and suspended sediment. The combined effects of seasonal wind patterns and submerged seagrass density variation on sediment resuspension on subtidal flats need to be better quantified, particularly if we are interested in quantifying sediment budgets or predicting future change.

To better resolve spatial variations of dynamic factors and understand the effects of seasonal seagrass growth and winds on hydrodynamics and sediment transport, we apply a relatively high-resolution (~70 m) hydrodynamic and sediment transport Delft3D model that includes coupling of seagrass effects on flow, waves, and sediment resuspension in a shallow coastal bay (South Bay) on Virginia's Atlantic coast. Rather than simply increasing bed roughness to parameterize attenuation of flow and waves, we used a more physically based approach to simulate vegetation effects on the mean flow and wave dissipation based on the approaches of Baptist et al. (2007) and Suzuki et al. (2012). The coupled model was then extensively validated using seasonal field hydrodynamic and suspended sediment data within a seagrass meadow and a nearby unvegetated site. We used the model to quantify seagrass effects on bay dynamics under: (1) typical summer conditions when seagrass density reaches a maximum and winds are predominantly southwesterly, and (2) winter conditions when frequent and stronger northeasterly winds coincide with minimum seagrass density. The results were analyzed to address three questions. (1) What are the effects of seasonal variations in seagrass density on hydrodynamics and sediment transport in a shallow coastal bay? (2) What are the relative contributions of flow retardation and wave attenuation in reducing sediment resuspension in seagrass meadows during summer and winter conditions? (3) How do rates and patterns of sediment erosion/deposition within seagrass beds vary in response to seasonal variations in wind and seagrass density? Our results underscore the tight coupling of vegetation interactions with physical environments in shallow coastal bays, provide useful guidance on the selection of vegetation parameters for coupled model simulations, and highlight the large variations in flow reduction, bed shear stress and net sediment accumulation that accompany small changes in density when meadow densities are low.

2 Materials and methods

2.1 Study area

This study was conducted in South Bay, a shallow coastal lagoon within the Virginia Coast Reserve (VCR) with an area of ~31.5 km^2. The VCR is a shallow coastal barrier-bay system located on the eastern shore of Virginia along the Atlantic side of the Delmarva Peninsula (Figure 1a) and is one of the 28 sites of the Long-Term Ecological Research (LTER) network. This system lacks significant fluvial freshwater and sediment input and is a mostly undeveloped area with low nutrient loading. Since local human impact on this coastal bay system is relatively small, the VCR provides a unique opportunity to study coastal system evolution under climate change (McGlathery et al., 2007).

South Bay has an average water depth of 1.0 m below mean sea level (Reidenbach & Thomas, 2018); a barrier island (Wreck Island) with back-barrier marsh borders its eastern side (Figure 1b). Tides within the bay are semidiurnal with a mean tidal range of 1.2 m. Wind activity shows a strong seasonal pattern in this region, with typical southerly winds during the summertime and more frequent and stronger northerly winds in winter (Fagherazzi and Wiberg, 2009; Figure 1c). Wind-generated waves are the dominant force driving sediment resuspension

and high suspended sediment concentration (SSC) in the shallow bays of the VCR (Lawson et al., 2007; Mariotti et al., 2010). South Bay is close to the southern geographical limit for eelgrass (*Zostera marina*) in the Western Atlantic (Aoki et al., 2020) and is a successful seagrass restoration site (McGlathery et al., 2013; Orth & McGlathery, 2012) with *Zostera marina* dominating the subtidal flats (Figure 1b). Maximum seagrass density occurs during summer with a peak density of approximately 400-550 shoots m^{-2}, while the minimum seagrass density is 50-100 shoots m^{-2} in winter due to senescence (Hansen & Reidenbach, 2013; Oreska et al., 2017; Reidenbach & Thomas, 2018; Rheuban et al., 2014). Because seagrass meadows can effectively trap fine particles, bed sediment in South Bay is dominated by very fine sand with a mean grain size of 71 μm (Lawson et al., 2007; Oreska et al., 2017).

2.2 Model descriptions

For this study, we used the process-based and spatially resolved hydrodynamic and sediment transport model Delft3D to simulate flow, waves, and sediment resuspension in the VCR. Delft3D is widely used and has been validated for various coastal environments (Apotsos et al., 2011; Dastgheib et al., 2008; Edmonds & Slingerland, 2010; Lesser et al., 2004). It solves the Navier-Stokes equations for an incompressible flow and advection-diffusion equation for multiple sediment fractions. The Delft3D model uses the Partheniades-Krone formulation to calculate cohesive sediment erosion and deposition fluxes (Lesser et al., 2004) and the Van Rijn et al. (2001) approach to estimate non-cohesive sediment transport. The Delft3D flow model can be coupled with the nearshore phase-averaged wave model SWAN to simulate flow-wave interaction. The SWAN model solves the wave action balance equation, which includes effects of wave generation, propagation, refraction, diffraction, dissipation and nonlinear wave-wave interactions (Booij et al., 1999), and passes wave parameters to the flow model to calculate combined wave-current bed shear stress.

To better resolve flow, sediment fluxes and vegetation effects in the core study area and to improve computational efficiency, we used the domain decomposition technique (Deltares, 2014) to locally refine the model grid size in South Bay and divided the overall model into two domains (Figure 1a). Parallel computations can be carried out on the large domain (resolution of 200 m) and small domain (resolution of ~70 m), and these two domains communicate and exchange information along their shared boundaries at each time step. Compared with previous hydrodynamic models applied in the VCR system (resolution of 250 m; Castagno et al., 2018; Nardin et al., 2018; Wiberg et al., 2015), the finer grid size (~70 m) of the small model domain is able to better resolve seagrass meadows (2×4 km) in South Bay and the bordering barrier island (0.7×5 km).

2.3 Coupling seagrass effects in Delft3D

In order to establish a process-based model to resolve flow-wave-vegetation-sediment interactions, vegetation effects on reduction in flow and waves were incorporated in Delft3D. Seagrass effects on flow were represented as submerged vegetation using the Baptist vegetation module in Delft3D (Baptist et al., 2007). The Baptist vegetation equation has been widely tested and validated by laboratory experiments and field measurements, and produced a good fit with those datasets (e.g., Arboleda et al., 2010; Crosato & Saleh, 2011). This method considers vegetation as cylindrical structures characterized by vegetation height (h_v), stem diameter (b_v), shoot density (N), and vegetation flow drag coefficient (C_D) and calculates the corresponding

vegetation drag (τ_v). The skin bed shear stress for sediment transport (τ_b) then can be obtained by subtracting the vegetation drag from total shear stress (τ_t). The Baptist vegetation module has been successfully applied in several depth-averaged Delft3D model studies to investigate vegetation effects on coastal environments, and was able to produce reasonable simulation results (Nardin et al., 2016, 2018; Nardin & Edmonds, 2014). In order to account for vegetation bending effects under mean flow conditions, we followed the approach of Dijkstra (2009) and used a deflected vegetation height that is reduced by approximately 20% of its typical value and a calibrated seagrass flow drag coefficient (C_D). Numerous previous studies have shown that the Baptist vegetation model can generate a very similar flow condition to flexible vegetation when using an appropriate deflected height and equivalent drag coefficient values (Hu et al., 2015; Lera et al., 2019; Nardin et al., 2018). More detailed descriptions of the vegetation module in the depth-averaged Delft3D model can be obtained from Nardin et al. (2018). Numerous wave models have been developed recently to quantify wave attenuation induced by coastal vegetation (e.g., Ma et al., 2013; Phan et al., 2019; van Rooijen et al., 2016; Wu et al., 2016). In this study, the vegetation wave energy dissipation model developed by Suzuki et al. (2012) was implemented in the SWAN model to simulate seagrass effects on waves. This approach adds a vegetation dissipation term which depends on vegetation height (h_v), stem diameter (b_v), shoot density (N), and vegetation wave drag coefficient ($\widetilde{C_D}$) into the wave action density spectrum balance equation. Recent studies (e.g., Baron-Hyppolite et al., 2018; Wu et al., 2016) have shown that this explicit vegetation representation in the SWAN model can produce reasonable simulation results that were in good agreement with field data and flume experiments.

2.4 Model settings and validation datasets

The model used a rectangular grid of 148 by 444 nodes for the large domain and 305 by 302 nodes for the small domain. The northern, southern and eastern boundaries of the large domain are open ocean boundaries that are forced with water levels extracted from the NOAA tide gauge record at Wachapreague (WA, ID: 8631044; Figure S1a, c). Adjustments of tidal amplitude and tidal phase are applied at the boundaries (dampened by a factor of 0.9 and delayed 66 min; similar approach as Castagno et al., 2018) to generate the best tidal simulation results for the shallow bays. The flow model was coupled with the SWAN model every 60 minutes. Hourly wind conditions from the nearby NOAA station CHLV2 (Figure S1b, d) were used to drive the wave simulation and a uniform Collins bottom friction coefficient of 0.1 was used in SWAN.

Model bathymetry and high-resolution maps of bottom sediment size distributions (two mud components and one sand fraction) were extracted from Wiberg et al. (2015). The mud components comprise a 32–64 μm coarse silt fraction with a settling velocity of 3.6 mm s^{-1} and a <32 μm size fraction with a representative floc settling velocity of 0.75 mm s^{-1} (Wiberg et al., 2015). The critical shear stress for cohesive sediment erosion was set to 0.03 N m^{-2} (Lawson et al., 2007; Reidenbach & Thomas, 2018; Reidenbach & Timmerman, 2019). For the sand fraction, a representative median grain size of 125 μm was used. Since seagrass meadows can effectively trap fine sediment and modify bottom sediment size, sediment size distributions in South Bay seagrass meadows were initialized based on local measurements from Oreska et al. (2017). A spatially and temporally constant Chézy bed roughness of 50 $m^{1/2}s^{-1}$ was used in both model domains. The active sediment layer thickness that can affect sediment availability during each individual time step was set to 5 cm.

The model was initially run for two time periods, January 1-31 and June 1-30, 2011, with typical seasonal seagrass characteristics based on previous observations in South Bay (Table 1; Hansen & Reidenbach, 2013; Oreska et al., 2017; Reidenbach & Thomas, 2018; Rheuban et al., 2014). An initial smoothing time of 60 h was used to improve flow stability when the model started. Four transects (North, East, South, and West) were designed in the small domain to monitor water and sediment fluxes into and out of the seagrass meadows (Figure 1b). Because our study site is relatively shallow with a mean depth of ~1 m and well mixed, with little evidence of stratification or strong shear within the water column, we assume that the vertical structure of velocity has a relatively small impact on the general flow and sediment transport patterns. Therefore, the coupled model was implemented in depth-averaged mode with a time step of 0.25 min to reduce computational time. Six model scenarios were considered in our simulations (Table 2) to differentiate the effects of seagrass on flow and waves during different seasons. These model runs were forced with the same hourly measurements of tide, wind, and waves but had different vegetation settings. Model runs W1 and S1 were run without seagrass effects in winter and summer, respectively. Seagrass effects on flow were included in model runs W2 and S2. Model runs W3 and S3 were run with seagrass effects on flow and waves using winter and summer seagrass characteristics, respectively.

Time series of water depth, velocity, significant wave height (Hs), and SSC collected at a reference bare site and a seagrass site (see locations in Figure 1b) during each simulation period in 2011 were compared with simulation results output from model runs W3 and S3 for model validation. More detailed descriptions of the data collection and instrument configuration can be found from Hansen & Reidenbach (2018). The model simulated depth-averaged velocity at the bare site was converted to the velocity at 0.5 m above seabed using a logarithmic velocity profile distribution (Deltares, 2014) and compared with velocity measurements at the same height. Since the mean depth of the validation sites is small (<1 m) and the SSC in the water column does not show a strong vertical gradient (less than 5 mg L^{-1} between 0.1 m and 0.5 m above seabed based on measurement results), we assumed that the SSC measured at 0.5 m above seabed was roughly equal to depth-averaged SSC in model validation. Time series of measured SSC collected at both sites in June 2011 showed persistently high values (~30 mg L^{-1}) that were unrelated to current and wave strength. This high background turbidity is likely caused by episodically high chlorophyll concentrations in the water column during summer. A recent study by Reidenbach & Timmerman (2019) found that water column chlorophyll levels at the study site reached a maximum in June when seagrass density was high. Considering that the focus of this study is vegetation interaction with physical processes, we did not attempt to model biologically induced background turbidity levels in our model validation.

3 Results

3.1 Model sensitivity tests and validation

A series of model runs were carried out to test the sensitivity of flow-wave-vegetation interactions to variations in vegetation height, shoot density, and vegetation drag coefficients (Figure S2). Typical summer vegetation characteristics (h_v= 0.4 m, b_v = 0.4 cm, N = 400 shoots m^{-2}; Table 1) were set as our reference case in the calibration. In each set of calibration runs, only one vegetation parameter was changed while other parameters remained constant. The calibration results show that vegetation interaction with flow and waves is non-linear with rapid changes as a function of shoot density at low densities but little change in flow retardation after

vegetation density reaches some critical value (≥400 shoots m^{-2} for our study site). Sediment resuspension is sensitive to shoot density and the wave drag coefficient for vegetation. Seagrass-related drag coefficients for flow and waves were used as calibration factors to match model results with seasonal field measurements. A seagrass flow drag coefficient of 0.4 (0.2) in summer (winter) produced best agreement between model results and measurements. A constant seagrass wave-drag coefficient of 3.0 was applied in both simulation periods.

The model simulated water levels in each period were checked against measured water levels at our tidal reference site at Wachapreague (WA, Figure S3). R-squared (R^2) and Root Mean Square Error (RMSE) were calculated for each simulation. Good agreement was obtained in January (R^2= 0.98, RMSE = 0.07 m) and in June (R^2= 0.99, RMSE = 0.05 m). The model results of run W3 and run S3 were validated using seasonal field hydrodynamic and suspended sediment data during a 4-day period in 2011 from a bare site and a seagrass site in South Bay (Figure 2 & Figure 3; for detailed validation datasets, please refer to Hansen & Reidenbach, 2018). Model skill indices (bias, RMSE, and Willmott Skill Index) were calculated to quantify model ability to characterize hydrodynamic and suspended sediment characteristics in South Bay (Table 3). The skill index proposed by Willmott (1981) is defined as

$$Skill = 1 - \frac{\sum|X_{model} - X_{obs}|^2}{\sum(|X_{model} - \overline{X_{obs}}| + |X_{obs} - \overline{X_{obs}}|)^2} \quad (1)$$

where X_{model} and X_{obs} are the model predicted variables and observations, respectively, and $\overline{X_{obs}}$ is the time mean observation value. A skill of one indicates perfect agreement between model results and observations, while a skill of zero shows complete disagreement.

Model predicted water levels slightly over-estimated measured levels in South Bay, with a positive bias less than 0.10 m; RMSE was lower than 0.16 m during each period and skill scores were very high (≥0.94). Despite similar wave height RMSE values at both sites, wave height skill scores for the seagrass site (0.87 & 0.67) were generally higher than those of bare site (0.68 & 0.56). The model did not reproduce the wave height peaks on January 21 and June 19 at the bare site (Figure 2b, d). The discrepancy for the first event was due to low wind speed input for the wave model. Although wave height measurements showed Hs ≥0.3 m during this period (Figure 2b), local wind speed records of CHLV2 station were too small (<5 m s^{-1}) to generate such a wave event. Either spatially variable wind conditions or local amplification of wave conditions during that time could be responsible for the disagreement. The model over-predicted bare site Hs on June 19 when the winds came from the south with a wind speed of ~8 m s^{-1}. Based on the results of a preliminary model sensitivity test of wind direction impacts on Hs, southerly winds had a relatively large wind fetch for our study site, but the observation records only showed a small wave height peak during the same period. We speculate that this disagreement may have been caused by high density seagrass surrounding the bare site in summer that altered the wave pattern in the bay. The best skill score for modeled velocity was at the bare site in January (0.84); the skill scores were lower at the bare site (0.69) and seagrass site (0.58) in June when seagrass density reached its maximum. In general, model-predicted velocity captures the stronger peak velocity during ebb tides but over-estimates peak velocity during flood tides (Figure 2e, g & Figure 3f). The total modeled SSC was calculated by summing the SSC of each sediment component output from the model. Our simulation results show that the SSC in the seagrass meadow area was dominated by the <32 μm size fraction (contributing to >95% of total SSC variations). Therefore, we did not attempt to further separate the

contribution of each sediment fraction but only show the results of total SSC (hereafter referred to as the "SSC") in the following text. Skill scores for SSC were high in January at the bare site (0.80) and seagrass site (0.82). The model successfully captured most sediment resuspension events (Figure 2f & Figure 3e). Although direct validation of the summer SSC was not available at both sites, the summer SSC levels predicted by the model (Figure 2h & Figure 3g) were consistent with our SSC measurements inside and outside the seagrass meadow during the summer of 2019 when background turbidity was low (Figure S4). Sediment resuspension was greatly reduced in the seagrass meadow compared with the nearby unvegetated site during summer when seagrass density was high. Considering the inherent complexity of natural environments and the somewhat simplified dynamics of flow-wave-vegetation-sediment interactions as represented in the model, we believe that the discrepancy between observations and our model predictions is acceptable and this coupled model is able to produce reasonable simulations of these interactions under varying forcing and vegetation densities in our study system.

3.2 Seasonal seagrass effects on hydrodynamics

Numerous field measurements (e.g., Hansen & Reidenbach, 2013; Hasegawa et al., 2008; Reidenbach & Thomas, 2018) have shown that high-density seagrass in summer resulted in much larger reductions in flow and waves compared with winter meadows. This seasonal seagrass control on flow and waves was also predicted by our model. Comparison of modeled depth averaged velocity and Hs between the bare site and seagrass site output from model run W3 shows that there was <10% reduction in flow and waves at vegetated sites during winter when seagrass density was at its minimum (Figure 4a, b). In contrast, seagrass meadows significantly attenuated flow (60%) and reduced wave height (20%) during late spring-early summer when its density reached a maximum (model run S3; Figure 4a, b). Depth averaged velocity remained low (<0.1 m s^{-1}) in the meadows when high density seagrass occupied the seabed, even at peak flood/ebb tides (Figure 5a). The difference of Hs between model runs S2 and S3 reveals that Hs could be reduced by 0.1 m in a storm event ($Hs \geq 0.3$ m) when wave attenuation effects caused by seagrass were included in the model (Figure 5b).

Cumulative water flux into the seagrass meadows was monitored through the model transects (Figure 1b) in each simulation period (January & June). There was no significant difference of water flux between model runs S2 (W2) and S3 (W3), indicating wave attenuation by seagrass had little effect on water flux into the meadows. Therefore, we only present results of model runs W1, W3, S1, and S3 here. The presence of seagrass had a strong seasonal impact on the water exchange with the seagrass meadows. During winter when seagrass density was low, flow reduction caused by seagrass was relatively weak, resulting in little change of cumulative water flux of each transect (W1 vs. W3 in Figure 6a). In contrast, cumulative water flux was reduced by ~70% in transects North, South, and West in model run S3 compared with model run S1 (Figure 6a). Although the net water flux into the seagrass meadows (the sum of water flux through four transects) remained relatively constant with/without seagrass flow effects in cases S1 and S3, the cumulative water flux through each transect was reduced significantly in S3 due to flow reduction by seagrass. As a result of velocity retardation, seagrass meadows in summer experienced less flushing by tidal flows (decrease by ~70%) compared with the non-vegetated case, which potentially increases the vulnerability of the coastal bay to pollution and heat stress by increasing water residence time in the meadows. Cumulative water flux was also influenced by seasonal wind patterns. Prevailing southerly winds in summer caused more water to enter the

system through the South transect and then discharge through the North transect to the region near the northern inlet of the bay, while northerly winds in winter kept pushing the water back into the bay, resulting in smaller water flux through the North transect than in summer (W1 and S1 in Figure 6a).

3.3 Seasonal seagrass effects on sediment transport

Seasonal growth and senescence of seagrass not only exerted a strong influence on attenuation of flow and waves, but also altered sediment resuspension on the flats. Model simulations show that the SSC was similar at both the bare site and seagrass site during winter when seagrass density was at its minimum (Figure 4c). However, SSC at the seagrass site was decreased by 85% in summer when seagrass density reached a maximum (Figure 4c), indicating that high density seagrass can effectively inhibit sediment resuspension. Spatial distributions of total SSC in model runs S1 and S3 during a storm event clearly demonstrate this strong seasonal control of seagrass on sediment resuspension (Figure 7). Without seagrass effects on flow and waves in model run S1, fine sediment in seagrass meadows was easily resuspended into the water column (Figure 7a). Once seagrass effects were included in model run S3, there was almost no sediment resuspension within the seagrass meadows and SSC was decreased significantly due to strong attenuation of flow and waves by high density seagrass, even during a storm event (Figure 7b).

Simulated sediment fluxes into and out of the seagrass meadow were calculated at each of the monitoring transects (Figure 6b). The results show that seagrass meadows trapped sediment in the bay during summer when seagrass density was high, with a net cumulative sediment input of 3.4×10^3 tons (S3 in Figure 6b). During winter when attenuation of flow and waves caused by seagrass was relatively weak, the seagrass meadows maintained a nearly balanced sediment budget (-2.7×10^2 tons; W3 in Figure 6b). In contrast, significant sediment output from the seagrass meadows was found in both simulation periods when seagrass effects were not included in the model (W1 and S1 in Figure 6b). The corresponding sediment fluxes were -9.5×10^3 tons and -6.1×10^3 tons, respectively; the flux was larger in winter as there were more frequent and stronger northerly winds during that period. Therefore, vegetation effects are critical for this system to maintain a depositional state, with low density winter seagrass providing significant reductions in sediment loss compared to completely unvegetated conditions.

4 Discussion

4.1 Non-linear effects of seasonally varying seagrass density on flow

Seasonal growth and senescence of seagrass exerted a strong influence on flow patterns and water exchange at our study site (Figure 4a, 5a, 6a). The main factor controlling this seasonal pattern is variation in seagrass shoot density, which reached a maximum ($\geq$400 shoots m^{-2}) during late spring-early summer and decreased to a minimum (50-100 shoots m^{-2}) in winter. Analysis of normalized velocity at the seagrass site (the ratio of depth averaged velocity with seagrass effects to the velocity in a completely unvegetated simulation) as a function of seagrass density (Figure 8a) illustrates that the most rapid changes of velocity occurred at low seagrass densities, with normalized velocity decreasing by 40% as density increases from 25 to 200 shoots m^{-2}. Once seagrass density exceeded 400 shoots m^{-2}, there was little change in flow reduction (<7% of velocity change in the range from 400 to 800 shoots m^{-2}). Similarly,

normalized bed shear stress at the seagrass site (the ratio of bed shear stress with seagrass effects to the bed shear stress in a completely unvegetated simulation) was reduced by ~90% within the low density range (0-200 shoots m^{-2}; Figure 8b), but by less than 5% once seagrass density ≥400 shoots m^{-2}. Our calibration results also show that depth averaged velocity decreased non-linearly with increasing vegetation height and vegetation drag coefficient (Figure S2).

The model prediction of velocity reduction at high seagrass densities agrees with previous flume studies regarding the limit of flow reduction when seagrass density is above certain thresholds (Gambi et al., 1990; Ganthy et al., 2015; Peralta et al., 2008). Higher shoot density increased the magnitude of velocity reduction when densities were moderate. However, this flow reduction effect reached a limit at the point when flow velocity was completely attenuated within the vegetation canopy due to a high shoot density above a threshold value (Peralta et al., 2008). Widdows and Brinsley (2002) reported a similar non-linear density dependent relationship between depth averaged velocity and stem density in their flume experiments with marsh vegetation (*Spartina anglica*). Their high-density threshold (~400 shoots m^{-2}) was similar to our model predicted results (Figure 8a), but the velocity reduction (75%) within the low-density range in their flume experiment was slightly higher than that predicted by our model (60%). Once the density threshold was reached, the velocity within the canopy decreased to almost zero, resulting in a skimming flow above the canopy.

The presence of high-density seagrass not only attenuated flow within the meadow, but also affected flow patterns outside the meadow. Velocity differences between non-vegetated case S1 and vegetated case S3 during peak ebb show that flow reduction occurred upstream and in the wake of the meadow (Figure 9a). Velocity reduction in these areas (~20%) was smaller than the reduction within the meadow (~60%). Due to flow obstruction by the seagrass meadow, tidal flow was deflected around the meadow and concentrated at the western edge (Figure 9a), resulting in flow velocity increasing by 30% at the meadow edge and water flux through the adjacent tidal channel increasing by 12% (Figure 9b). Flow enhancement outside the meadow, however, was not able to offset diminished water fluxes within the meadow, resulting in a 10% decrease of total water flux through the monitoring transect (Figure 9b). This flow acceleration and deceleration pattern caused by seagrass meadows was also reported by Beudin et al. (2017). In their rigid vegetation case, an idealized square seagrass meadow (1 km by 1 km) in the shallow basin induced an 80% reduction of depth averaged velocity in its wake and an 40% increase of depth averaged velocity at the edge. Similarly, Lera et al. (2019) found that seagrass meadows produced a lateral velocity amplification around a river mouth bar covered by dense seagrass, and this lateral velocity amplification increased with seagrass height and density. At a larger spatial scale, Nardin et al. (2018) found that salt marsh and seagrass in the VCR system could slightly increase the velocity at the tidal inlets by 2% in their most vegetated case (with double density and vegetation height).

4.2 Contributions of attenuation of flow and waves in reducing sediment resuspension

The impact of seagrass on trapping fine-grained particles from the water column and reducing sediment resuspension is the most important positive feedback for seagrass growth, as it increases light penetration to the seabed and stimulates seagrass growth (Carr et al., 2010; De Boer, 2007). Despite significant variability in bed shear stress and SSC due to changes in flow velocity and wave conditions in response to tides and storms, seasonal seagrass growth and

senescence has been shown to exert a strong control on sediment resuspension within seagrass meadows (Gacia & Duarte, 2001; Ganthy et al., 2013; Hansen & Reidenbach, 2013).

Our model simulations show that high density seagrass meadows can effectively attenuate flow (60%) and reduce wave height (20%) during late spring-early summer, resulting in a decrease in bed shear stress and SSC levels (85%), while there was no significant difference in SSC between the seagrass site and the unvegetated site in winter due to weak attenuation of flow and waves under low seagrass density conditions (Figure 4). This seasonal seagrass control on sediment resuspension was also captured by previous in situ hydrodynamic and SSC measurements in South Bay. These studies showed that seagrass meadows resulted in >50% reduction in flow velocity (Hansen & Reidenbach, 2012, 2013) and approximately 30-50% attenuation in wave height (Reidenbach & Thomas, 2018; only waves that propagated in a limited range of north to south directions were included in their analysis) in summer when seagrass density was high; the resultant bed shear stresses rarely exceeded the critical shear stress to initiate sediment resuspension during the same period (Reidenbach & Timmerman, 2019). In contrast, similar dynamic conditions and SSC levels were found at both vegetated and unvegetated sites in winter (Reidenbach & Timmerman, 2019), indicating relatively weak vegetation control on sediment resuspension during the senescence period.

Both flow retardation and wave attenuation caused by seagrass contribute to reductions in sediment resuspension. However, it is difficult to quantify the relative contribution of each process in inhibiting sediment resuspension from in situ measurements because of the non-linear interaction between waves and currents (Jing & Ridd, 1996) and the lack of direct measurements of waves and currents in the wave boundary layer within a seagrass meadow (De Boer, 2007; Reidenbach & Thomas, 2018). One of the advantages of using a coupled model is it makes it possible to separate attenuation of flow and waves on sediment resuspension within seagrass meadows. Probability density distributions of combined wave-current bed shear stress at the seagrass site were calculated for each model run (Figure 10). When seagrass effects were not included in the model (W1 & S1), stronger wind waves in winter (Figure 1c) resulted in larger bed shear stresses (mean τ_b = 0.70 N m^{-2}) than in summer (mean τ_b = 0.51 N m^{-2}). Reductions in bed shear stress during summer were mainly caused by flow retardation (Figure 10b). Flow retardation alone reduced mean wave-current bed shear stress from 0.51 N m^{-2} to 0.08 N m^{-2} (S1 vs. S2, Figure 10b); including effects of wave attenuation further reduced bed shear stress to a mean value of 0.05 N m^{-2} (S3, Figure 10b). Low densities of seagrass in winter were sufficient to lower bed shear stresses by flow retardation (W1 vs. W2, Figure 10a), though the reductions were much smaller than in summer. Wave attenuation had little effect on bed shear stress at low seagrass densities (W2 vs. W3, Figure 10a). Although there has been little quantitative analysis on the relative contribution of flow retardation and wave attenuation in inhibiting sediment resuspension in seagrass bed, our findings based on probability density distributions of combined bed shear stress agree with the one-year observation reported by Hasegawa et al. (2008) in the Akkeshi-ko estuary, Japan. By applying sediment traps in the seagrass meadow, they found that sediment resuspension was closely related to flow reduction caused by seagrass canopy and thereby varying with seasonal seagrass growth and senescence, while sediment resuspension was not correlated with wind speed.

4.3 Seasonal sediment transport and deposition

Sediment accumulates within a seagrass meadow when deposition of suspended sediment is greater than local resuspension. Although previous studies have shown that seagrasses can effectively trap sediment and promote sediment deposition (Gacia et al., 1999, 2003; Gacia & Duarte, 2001; Ganthy et al., 2013, 2015), there are few direct observations of spatial erosion and deposition patterns within seagrass beds, and most of those focus on sediment grain size changes associated with seagrass (Chen et al., 2007; van Katwijk et al., 2010).

Our model results illustrate that seasonal seagrass variations had a strong impact on spatial patterns of erosion and deposition within seagrass meadows. Erosion was found just outside the western edge of the meadow in both simulation periods (Figure 11a, b) due to flow concentration at the edges (Beudin et al., 2017; Lera et al., 2019). During summer when seagrass density was high, slight erosion of the seagrass bed (~1 mm) was observed in some areas in the central meadow that had a shallower depth, while pronounced sediment accumulation (> 6 mm) occurred at the edges of the seagrass bed where reduced bed shear stresses allowed deposition of suspended sediment that was transported into the meadow (Figure 11b). The spatial erosion and deposition pattern near the meadow edges in our simulation was consistent with other model results considering seagrass meadow edge effects (Carr et al., 2016; Chen et al., 2007). These models predicted similar local scouring just outside the meadow and enhanced sediment deposition near the edges within the meadow. Our summer simulation results also show that sediment deposition was closely related to distance into the seagrass meadow. The amount of deposition decreased logarithmically with distance into the bed until the advective sediment source was depleted (Figure 12). When interpreting sediment deposition patterns within seagrass meadows or comparing sediment accumulation rates among different systems, it is important to consider the effects of multiple factors (e.g., different sampling location and depth, advective sediment supply, and the dependence of deposition on distance into the meadow), which may help explain the low depositional rates within the seagrass meadows during summer growth season obtained by previous studies (e.g., Gacia & Duarte, 2001).

During winter when low seagrass density coincided with stronger northerly winds, sediment resuspension was enhanced (Figure 4c) and a more varied pattern of erosion and deposition was found on the seagrass beds. While sediment deposition still occurred at the edges of the meadow, erosional areas expanded and severe erosion (>5 mm) was found in the central meadow (Figure 11a). Low densities of seagrass allowed suspended sediment to be transported further into the meadow, resulting in regions of interior deposition in the southern portion of the meadow where larger water depths and smaller bed shear stresses promoted sediment deposition (Figure 11a). Unlike the relatively large and stable reduction in velocity and shear stress associated with high seagrass density in summer, flow conditions associated with low seagrass densities were more variable. Within the range of 25-200 shoots m^{-2}, the normalized bed shear stress in our flow simulations decreased from 0.4 to 0.1, a 75% reduction in bed shear stress (Figure 8b).

When seagrass shoot density was low in winter, small changes of density could result in strong variations in net sediment flux into/out of the meadow (Figure 13). The seagrass meadow maintained a nearly balanced sediment budget during winter when stem density = 50 shoots m^{-2} (-2.7×10^2 tons; W3 in Figure 6b). Higher winter seagrass densities gradually increased net sediment input to the meadow (>60 shoots m^{-2} in Figure 13). However, if seagrass meadows were present in much lower densities (<50 shoots m^{-2} in Figure 13; W1 and S1 in Figure 6b) or

was broadly lost from the bay as happened in the 1933 pandemic (Orth & McGlathery, 2012), the meadow area would inevitably become erosional, leading to dramatic sediment export as densities approached zero. Similarly, massive sediment loss was reported in Barnegat Bay, USA, as a result of a rapid decline in the extent of seagrass meadows within the bay system (Donatelli et al., 2018). The strong variations in flow conditions and sediment flux associated with low winter seagrass density could have a significant impact on light availability for seagrass growth, organic matter burial, and ecosystem metabolism during the senescence period (Carr et al., 2010; Lawson et al., 2012; Rheuban et al., 2014) and strongly alter annual sediment budgets and long-term dynamics of seagrass ecosystems. Considering that most previous research has focused on flow dynamics during summer when seagrass is under full-growth conditions (De Boer, 2007), more comprehensive seasonal investigations of seagrass interactions with physical environments are needed.

4.4 Model limitations

Our coupled model was able to produce reasonable simulations of flow-wave-vegetation-sediment interactions under varying forcing and vegetation densities using spatially uniform seasonal vegetation inputs. However, this uniform vegetation approach may not be able to reproduce some heterogeneous patterns observed within seagrass meadows associated with spatial gradients in seagrass density, such as spatially variable accretion rates (Ganthy et al., 2013). Moreover, our model grid size (~70 m) was too coarse to resolve seagrass patchiness (usually on a scale of several meters), which has been shown to impact the distributions of bed shear stress and sediment transport rates, and consequent light environments for seagrass growth (Carr et al., 2016; Shan et al., 2020).

Another limitation of this study is the absence of vegetation dynamics in model simulations. We used representative seagrass characteristics in each period (January & June) to quantify the seasonal impacts of seagrass on flow and sediment dynamics and neglected organic matter accumulation. A more realistic approach is to simulate continuous vegetation growth and organic matter production over an annual cycle, along with vegetation interactions with the physical environment. Several studies have successfully integrated a vegetation growth module in their hydrodynamic and sediment transport simulations, either by considering vegetation growth as a function of water temperature and available photosynthetically active radiation (Carr et al., 2010), or applying a vegetation population dynamics approach that depends on vegetation colonization, growth, mortality, and interactions with hydro morphodynamic processes (Best et al., 2018; Brückner et al., 2019). These studies show that including vegetation growth dynamics and bio-accumulation can better characterize ecomorphodynamic processes and improve model predictive capabilities for future changes.

5 Conclusion

In this study, we coupled seagrass effects on flow, waves, and sediment resuspension in a spatially resolved Delft3D model and applied it in a shallow coastal bay on Virginia's Atlantic coast to better understand the effects of seasonal seagrass growth on flow and sediment dynamics. Our simulation results show that seasonal seagrass growth and senescence exerted a strong influence on bay dynamics: dense seagrass during summer significantly attenuated flow (60%) and waves (20%) and reduced SSC (85%); low-density seagrass in winter had limited effects on attenuation of flow and waves, resulting in similar SSC between the seagrass site and

the unvegetated site. As a result of velocity reduction, seagrass meadows in summer experienced less flushing by tidal flows (decrease by ~70%), which potentially increases its vulnerability to pollution and heat stress by increasing water residence time in the meadows.

Model results demonstrate that the vegetation effects on flow are non-linear. Higher seagrass density increased the magnitude of flow reduction until a density threshold (400 shoots m^{-2}) was reached, which is consistent with previous flume studies regarding the limit of flow reduction by seagrass (Gambi et al., 1990; Ganthy et al., 2015; Peralta et al., 2008). Due to flow obstruction by the seagrass meadows, tidal flow was deflected around the meadow and concentrated at the western edge. Although flow velocity increased by 30% at the meadow edges, it was not able to offset the loss of water flux within the meadow and the total water flux discharged through the cross-meadow transect was reduced by 10%. While difficult to measure, the detailed hydrodynamics resolved in the model allowed us to separate the relative contributions of flow retardation and wave attenuation to reductions of bed shear stress in seagrass meadows. We found that 85% of the decrease in bed shear stress during summer was caused by flow retardation.

Seasonal seagrass variations had a strong impact on spatial patterns of erosion and deposition within seagrass meadows. Erosion was found just outside the western edge of the meadow in each season due to flow concentration at the edges. During summer when seagrass density was high, pronounced sediment accumulation (>6 mm/month) occurred at the edges of the seagrass bed and decreased logarithmically with distance into the meadow. During winter when low seagrass densities coincided with stronger northerly winds, sediment resuspension was enhanced, and severe erosion (>5 mm/month) was found in the central, shallower part of the meadow.

Unlike the relatively large and stable reduction in velocity and shear stress associated with high seagrass density in summer, flow conditions associated with low seagrass densities during the senescence period were more variable. When seagrass shoot density was low in winter, a small change of density could result in strong changes in net sediment flux into/out of the meadow. The strong variations in flow conditions and sediment flux associated with variations in winter seagrass densities could have a significant impact on light availability for seagrass growth, organic matter burial, and ecosystem metabolism.

Acknowledgements

Primary support for this work was provided by the National Science Foundation (NSF) through the VCR LTER award 1832221 and Coastal SEES award 1427282. M. Reidenbach was supported by NSF award 1151314. Logistical support was provided by the staff and facilities at the Anheuser-Busch Coastal Research Center. The developers of Delft3D are acknowledged for open access to their code. We would like to thank the editor Ryan P. Mulligan and two anonymous reviewers for valuable suggestions that improved the manuscript. Model validation data in this work are available in the NSF LTER data repository (https://doi.org/10.6073/pasta/33682bfc1bdcdef08c9948560177338c).

References

Aoki, L. R., McGlathery, K. J., Wiberg, P. L., & Al-Haj, A. (2020). Depth Affects Seagrass Restoration Success and Resilience to Marine Heat Wave Disturbance. *Estuaries and Coasts*, *43*(2), 316–328. https://doi.org/10.1007/s12237-019-00685-0

Apotsos, A., Jaffe, B., & Gelfenbaum, G. (2011). Wave characteristic and morphologic effects on the onshore hydrodynamic response of tsunamis. *Coastal Engineering*, *58*(11), 1034–1048. https://doi.org/https://doi.org/10.1016/j.coastaleng.2011.06.002

Arboleda, A. M., Crosato, A., & Middelkoop, H. (2010). Reconstructing the early 19th-century Waal River by means of a 2D physics-based numerical model. *Hydrological Processes*, *24*(25), 3661–3675. https://doi.org/10.1002/hyp.7804

Baptist, M. J., Babovic, V., Uthurburu, J. R., Keijzer, M., Uittenbogaard, R. E., Mynett, A., & Verwey, A. (2007). On inducing equations for vegetation resistance. *Journal of Hydraulic Research*, *45*(4), 435–450. https://doi.org/10.1080/00221686.2007.9521778

Baron-Hyppolite, C., Lashley, C., Garzon, J., Miesse, T., Ferreira, C., & Bricker, J. (2018). Comparison of Implicit and Explicit Vegetation Representations in SWAN Hindcasting Wave Dissipation by Coastal Wetlands in Chesapeake Bay. *Geosciences*, *9*(1), 8. https://doi.org/10.3390/geosciences9010008

Best, S. N., Van der Wegen, M., Dijkstra, J., Willemsen, P. W. J. M., Borsje, B. W., & Roelvink, D. J. A. (2018). Do salt marshes survive sea level rise? Modelling wave action, morphodynamics and vegetation dynamics. *Environmental Modelling and Software*, *109*, 152–166. https://doi.org/10.1016/j.envsoft.2018.08.004

Beudin, A., Kalra, T. S., Ganju, N. K., & Warner, J. C. (2017). Development of a coupled wave-flow-vegetation interaction model. *Computers and Geosciences*, *100*, 76–86. https://doi.org/10.1016/j.cageo.2016.12.010

Booij, N., Ris, R. C., & Holthuijsen, L. H. (1999). A third-generation wave model for coastal regions 1. Model description and validation. *Journal of Geophysical Research: Oceans*, *104*(C4), 7649–7666. https://doi.org/10.1029/98JC02622

Brückner, M. Z. M., Schwarz, C., Dijk, W. M., Oorschot, M., Douma, H., & Kleinhans, M. G. (2019). Salt Marsh Establishment and Eco□Engineering Effects in Dynamic Estuaries Determined by Species Growth and Mortality. *Journal of Geophysical Research: Earth Surface*, *124*(12), 2962–2986. https://doi.org/10.1029/2019JF005092

Carr, J., D'Odorico, P., McGlathery, K., & Wiberg, P. (2010). Stability and bistability of seagrass ecosystems in shallow coastal lagoons: Role of feedbacks with sediment resuspension and light attenuation. *Journal of Geophysical Research: Biogeosciences*, *115*(3), G03011. https://doi.org/10.1029/2009JG001103

Carr, J. A., D'Odorico, P., McGlathery, K. J., & Wiberg, P. L. (2016). Spatially explicit feedbacks between seagrass meadow structure, sediment and light: Habitat suitability for seagrass growth. *Advances in Water Resources*, *93*, 315–325. https://doi.org/10.1016/j.advwatres.2015.09.001

Carr, Joel, Mariotti, G., Fahgerazzi, S., McGlathery, K., & Wiberg, P. (2018). Exploring the Impacts of Seagrass on Coupled Marsh-Tidal Flat Morphodynamics. *Frontiers in*

Environmental Science, *6*(SEP), 92. https://doi.org/10.3389/fenvs.2018.00092

Castagno, K. A., Jiménez-Robles, A. M., Donnelly, J. P., Wiberg, P. L., Fenster, M. S., & Fagherazzi, S. (2018). Intense Storms Increase the Stability of Tidal Bays. *Geophysical Research Letters*, *45*(11), 5491–5500. https://doi.org/10.1029/2018GL078208

Chen, S. N., Sanford, L. P., Koch, E. W., Shi, F., & North, E. W. (2007). A nearshore model to investigate the effects of seagrass bed geometry on wave attenuation and suspended sediment transport. *Estuaries and Coasts*, *30*(2), 296–310. https://doi.org/10.1007/BF02700172

Crosato, A., & Saleh, M. S. (2011). Numerical study on the effects of floodplain vegetation on river planform style. *Earth Surface Processes and Landforms*, *36*(6), 711–720. https://doi.org/10.1002/esp.2088

Dastgheib, A., Roelvink, J. A., & Wang, Z. B. (2008). Long-term process-based morphological modeling of the Marsdiep Tidal Basin. *Marine Geology*, *256*(1–4), 90–100. https://doi.org/10.1016/j.margeo.2008.10.003

De Boer, W. F. (2007). Seagrass-sediment interactions, positive feedbacks and critical thresholds for occurrence: A review. *Hydrobiologia*, 591(1), 5–24. https://doi.org/10.1007/s10750007-0780-9

Deltares. (2014). *Delft3D-FLOW User Manual (Version: 3.15.34158): Simulation of multi-dimensional hydrodynamic flows and transport phenomena, including sediments*.

Dijkstra, J. T. (2009). How to account for flexible aquatic vegetation in large-scale morphodynamic models. In *Coastal Engineering 2008* (pp. 2820–2831). World Scientific Publishing Company. https://doi.org/10.1142/9789814277426_0233

Donatelli, C., Ganju, N. K., Fagherazzi, S., & Leonardi, N. (2018). Seagrass Impact on Sediment Exchange Between Tidal Flats and Salt Marsh, and The Sediment Budget of Shallow Bays. *Geophysical Research Letters*, *45*(10), 4933–4943. https://doi.org/10.1029/2018GL078056

Donatelli, C., Ganju, N. K., Kalra, T. S., Fagherazzi, S., & Leonardi, N. (2019). Changes in hydrodynamics and wave energy as a result of seagrass decline along the shoreline of a microtidal back-barrier estuary. *Advances in Water Resources*, *128*, 183–192. https://doi.org/10.1016/j.advwatres.2019.04.017

Edmonds, D. A., & Slingerland, R. L. (2010). Significant effect of sediment cohesion on deltamorphology. *Nature Geoscience*, *3*(2), 105–109. https://doi.org/10.1038/ngeo730

Fagherazzi, S., & Wiberg, P. L. (2009). Importance of wind conditions, fetch, and water levels on wave-generated shear stresses in shallow intertidal basins. *Journal of Geophysical Research*, *114*(F3), F03022. https://doi.org/10.1029/2008JF001139

Fonseca, M., & Fisher, J. (1986). A comparison of canopy friction and sediment movement between four species of seagrass with reference to their ecology and restoration. *Marine Ecology Progress Series*, *29*, 15–22. https://doi.org/10.3354/meps029015

Fonseca, M. S., & Cahalan, J. A. (1992). A preliminary evaluation of wave attenuation by four species of seagrass. *Estuarine, Coastal and Shelf Science*, *35*(6), 565–576. https://doi.org/10.1016/S0272-7714(05)80039-3

Gacia, E., & Duarte, C. M. (2001). Sediment retention by a Mediterranean Posidonia oceanica meadow: The balance between deposition and resuspension. *Estuarine, Coastal and Shelf Science*, *52*(4), 505–514. https://doi.org/10.1006/ecss.2000.0753

Gacia, E., Granata, T. C., & Duarte, C. M. (1999). An approach to measurement of particle flux and sediment retention within seagrass (Posidonia oceanica) meadows. *Aquatic Botany*, *65*(1–4), 255–268. https://doi.org/10.1016/S0304-3770(99)00044-3

Gacia, E., Duarte, C. M., Marbà, N., Terrados, J., Kennedy, H., Fortes, M. D., & Tri, N. H. (2003). Sediment deposition and production in SE-Asia seagrass meadows. *Estuarine, Coastal and Shelf Science*, *56*(5–6), 909–919. https://doi.org/10.1016/S0272-7714(02)00286-X

Gambi, M., Nowell, A., & Jumars, P. (1990). Flume observations on flow dynamics in Zostera marina (eelgrass) beds. *Marine Ecology Progress Series*, *61*, 159–169. https://doi.org/10.3354/meps061159

Ganthy, F., Sottolichio, A., & Verney, R. (2013). Seasonal modification of tidal flat sediment dynamics by seagrass meadows of Zostera noltii (Bassin d'Arcachon, France). *Journal of Marine Systems*, *109–110*(SUPPL.), S233–S240. https://doi.org/10.1016/j.jmarsys.2011.11.027

Ganthy, Florian, Soissons, L., Sauriau, P.-G., Verney, R., & Sottolichio, A. (2015). Effects of short flexible seagrass *Zostera noltei* on flow, erosion and deposition processes determined using flume experiments. *Sedimentology*, *62*(4), 997–1023. https://doi.org/10.1111/sed.12170

Hansen, JCR, & Reidenbach, M. (2012). Wave and tidally driven flows in eelgrass beds and their effect on sediment suspension. *Marine Ecology Progress Series*, *448*, 271–287. https://doi.org/10.3354/meps09225

Hansen, JCR, & Reidenbach, M. (2013). Seasonal Growth and Senescence of a Zostera marina Seagrass Meadow Alters Wave-Dominated Flow and Sediment Suspension Within a Coastal Bay. *Estuaries and Coasts*, *36*(6), 1099–1114. https://doi.org/10.1007/s12237-013-9620-5

Hansen, Jennifer, & Reidenbach, M. (2018). Wave Dynamics and Fluid Stresses in Vegetated and Unvegetated Coastal Lagoons in Virginia, 2010-2011. *Virginia Coast Reserve Long-Term Ecological Research Project Data Publication Knb-Lter-Vcr.276.2*. https://doi.org/10.6073/PASTA/33682BFC1BDCDEF08C9948560177338C

Hasegawa, N., Hori, M., & Mukai, H. (2008). Seasonal changes in eelgrass functions: Current velocity reduction, prevention of sediment resuspension, and control of sediment-water column nutrient flux in relation to eelgrass dynamics. *Hydrobiologia*, *596*(1), 387–399. https://doi.org/10.1007/s10750-007-9111-4

Hu, K., Chen, Q., & Wang, H. (2015). A numerical study of vegetation impact on reducing storm surge by wetlands in a semi-enclosed estuary. *Coastal Engineering*, *95*, 66–76. https://doi.org/10.1016/j.coastaleng.2014.09.008

Jing, L., & Ridd, P. V. (1996). Wave-current bottom shear stresses and sediment resuspension in Cleveland Bay, Australia. *Coastal Engineering*, *29*(1–2), 169–186. https://doi.org/10.1016/S0378-3839(96)00023-3

Jones, C. G., Lawton, J. H., & Shachak, M. (1994). Organisms as Ecosystem Engineers. *Oikos*, *69*(3), 373. https://doi.org/10.2307/3545850

Koch, E., & Gust, G. (1999). Water flow in tide- and wave-dominated beds of the seagrass Thalassia testudinum. *Marine Ecology Progress Series*, *184*, 63–72. https://doi.org/10.3354/meps184063

Lawson, S., McGlathery, K., & Wiberg, P. (2012). Enhancement of sediment suspension and nutrient flux by benthic macrophytes at low biomass. *Marine Ecology Progress Series*, *448*, 259–270. https://doi.org/10.3354/meps09579

Lawson, S. E., Wiberg, P. L., McGlathery, K. J., & Fugatf, D. C. (2007). Wind-driven sediment suspension controls light availability in a shallow coastal lagoon. *Estuaries and Coasts*, *30*(1), 102–112. https://doi.org/10.1007/BF02782971

Lera, S., Nardin, W., Sanford, L., Palinkas, C., & Guercio, R. (2019). The impact of submersed aquatic vegetation on the development of river mouth bars. *Earth Surface Processes and Landforms*, *44*(7), 1494–1506. https://doi.org/10.1002/esp.4585

Lesser, G. R., Roelvink, J. A., van Kester, J. A. T. M. T. M., & Stelling, G. S. (2004). Development and validation of a three-dimensional morphological model. *Coastal Engineering*, *51*(8), 883–915. https://doi.org/https://doi.org/10.1016/j.coastaleng.2004.07.014

Ma, G., Kirby, J. T., Su, S. F., Figlus, J., & Shi, F. (2013). Numerical study of turbulence and wave damping induced by vegetation canopies. *Coastal Engineering*, *80*, 68–78. https://doi.org/10.1016/j.coastaleng.2013.05.007

Mariotti, G., Fagherazzi, S., Wiberg, P. L., McGlathery, K. J., Carniello, L., & Defina, A. (2010). Influence of storm surges and sea level on shallow tidal basin erosive processes. *Journal of Geophysical Research*, *115*(C11), C11012. https://doi.org/10.1029/2009JC005892

McGlathery, Karen, Reidenbach, M., D'Odorico, P., Fagherazzi, S., Pace, M., & Porter, J. (2013). Nonlinear Dynamics and Alternative Stable States in Shallow Coastal Systems. *Oceanography*, *26*(3), 220–231. https://doi.org/10.5670/oceanog.2013.66

McGlathery, KJ, Sundbäck, K., & Anderson, I. (2007). Eutrophication in shallow coastal bays and lagoons: the role of plants in the coastal filter. *Marine Ecology Progress Series*, *348*, 1–18. https://doi.org/10.3354/meps07132

Nagelkerken, I., Van Der Velde, G., Gorissen, M. W., Meijer, G. J., Van't Hof, T., & Den Hartog, C. (2000). Importance of mangroves, seagrass beds and the shallow coral reef as a nursery for important coral reef fishes, using a visual census technique. *Estuarine, Coastal and Shelf Science*, *51*(1), 31–44. https://doi.org/10.1006/ecss.2000.0617

Nardin, W., & Edmonds, D. A. (2014). Optimum vegetation height and density for inorganic sedimentation in deltaic marshes. *Nature Geoscience*, *7*(10), 722–726. https://doi.org/10.1038/NGEO2233

Nardin, W., Edmonds, D. A., & Fagherazzi, S. (2016). Influence of vegetation on spatial patterns of sediment deposition in deltaic islands during flood. *Advances in Water Resources*, *93*, 236–248. https://doi.org/10.1016/j.advwatres.2016.01.001

Nardin, W., Larsen, L., Fagherazzi, S., & Wiberg, P. (2018). Tradeoffs among hydrodynamics, sediment fluxes and vegetation community in the Virginia Coast Reserve, USA. *Estuarine, Coastal and Shelf Science*, *210*, 98–108. https://doi.org/10.1016/j.ecss.2018.06.009

Nepf, H. M. (2012). Flow and Transport in Regions with Aquatic Vegetation. *Annual Review of Fluid Mechanics*, *44*(1), 123–142. https://doi.org/10.1146/annurev-fluid-120710-101048

Oreska, M. P. J., McGlathery, K. J., & Porter, J. H. (2017). Seagrass blue carbon spatial patterns at the meadow-scale. *PLoS ONE*, *12*(4). https://doi.org/10.1371/journal.pone.0176630

Orth, R., & McGlathery, K. (2012). INTRODUCTION Eelgrass recovery in the coastal bays of the Virginia Coast Reserve, USA. *Marine Ecology Progress Series*, *448*, 173–176. https://doi.org/10.3354/meps09596

Orth, R. J., Carruthers, T. J. B., Dennison, W. C., Duarte, C. M., Fourqurean, J. W., Heck, K. L., et al. (2006). A Global Crisis for Seagrass Ecosystems. *BioScience*, *56*(12), 987–996. https://doi.org/10.1641/0006-3568(2006)56[987:agcfse]2.0.co;2

Paul, M., Bouma, T., & Amos, C. (2012). Wave attenuation by submerged vegetation: combining the effect of organism traits and tidal current. *Marine Ecology Progress Series*, *444*, 31–41. https://doi.org/10.3354/meps09489

Peralta, G., van Duren, L., Morris, E., & Bouma, T. (2008). Consequences of shoot density and stiffness for ecosystem engineering by benthic macrophytes in flow dominated areas: a hydrodynamic flume study. *Marine Ecology Progress Series*, *368*, 103–115. https://doi.org/10.3354/meps07574

Phan, K. L., Stive, M. J. F., Zijlema, M., Truong, H. S., & Aarninkhof, S. G. J. (2019). The effects of wave non-linearity on wave attenuation by vegetation. *Coastal Engineering*, *147*, 63–74. https://doi.org/10.1016/j.coastaleng.2019.01.004

Reidenbach, M. A., & Thomas, E. L. (2018). Influence of the Seagrass, Zostera marina, on Wave Attenuation and Bed Shear Stress Within a Shallow Coastal Bay. *Frontiers in Marine Science*, *5*(OCT), 397. https://doi.org/10.3389/fmars.2018.00397

Reidenbach, M. A., & Timmerman, R. (2019). Interactive Effects of Seagrass and the Microphytobenthos on Sediment Suspension Within Shallow Coastal Bays. *Estuaries and Coasts*, *42*(8), 2038–2053. https://doi.org/10.1007/s12237-019-00627-w

Rheuban, J. E., Berg, P., & McGlathery, K. J. (2014). Ecosystem metabolism along a colonization gradient of eelgrass (*Zostera marina*) measured by eddy correlation. *Limnology and Oceanography*, *59*(4), 1376–1387. https://doi.org/10.4319/lo.2014.59.4.1376

Shan, Y., Zhao, T., Liu, C., & Nepf, H. (2020). Turbulence and bed-load transport in channels with randomly distributed emergent patches of model vegetation. *Geophysical Research Letters*, e2020GL087055. https://doi.org/10.1029/2020gl087055

Suzuki, T., Zijlema, M., Burger, B., Meijer, M. C., & Narayan, S. (2012). Wave dissipation by vegetation with layer schematization in SWAN. *Coastal Engineering*, *59*(1), 64–71. https://doi.org/10.1016/j.coastaleng.2011.07.006

van Katwijk, M. M., Bos, A. R., Hermus, D. C. R., & Suykerbuyk, W. (2010). Sediment modification by seagrass beds: Muddification and sandification induced by plant cover and

environmental conditions. *Estuarine, Coastal and Shelf Science*, *89*(2), 175–181. https://doi.org/10.1016/J.ECSS.2010.06.008

Van Rijn, L. C., Roelvink, J. A., & Horst, W. ter. (2001). Approximation formulae for sand transport by currents and waves and implementation in DELFT-MOR. Z3054.

van Rooijen, A. A., McCall, R. T., van Thiel de Vries, J. S. M., van Dongeren, A. R., Reniers, A. J. H. M., & Roelvink, J. A. (2016). Modeling the effect of wave-vegetation interaction on wave setup. *Journal of Geophysical Research: Oceans*, *121*(6), 4341–4359. https://doi.org/10.1002/2015JC011392

Waycott, M., Duarte, C. M., Carruthers, T. J. B., Orth, R. J., Dennison, W. C., Olyarnik, S., et al. (2009). Accelerating loss of seagrasses across the globe threatens coastal ecosystems. Proceedings of the National Academy of Sciences of the United States of America, 106(30), 12377–12381. https://doi.org/10.1073/pnas.0905620106

Wiberg, P. L., Carr, J. A., Safak, I., & Anutaliya, A. (2015). Quantifying the distribution and influence of non-uniform bed properties in shallow coastal bays. *Limnology and Oceanography: Methods*, *13*(12), 746–762. https://doi.org/10.1002/lom3.10063

Widdows, J, Pope, N., Brinsley, M., Asmus, H., & Asmus, R. (2008). Effects of seagrass beds (Zostera noltii and Z. marina) on near-bed hydrodynamics and sediment resuspension. *Marine Ecology Progress Series*, *358*, 125–136. https://doi.org/10.3354/meps07338

Widdows, John, & Brinsley, M. (2002). Impact of biotic and abiotic processes on sediment dynamics and the consequences to the structure and functioning of the intertidal zone. *Journal of Sea Research*, *48*(2), 143–156. https://doi.org/10.1016/S1385-1101(02)00148-X

Willmott, C. J. (1981). On the validation of models. *Physical Geography*, *2*(2), 184–194. https://doi.org/10.1080/02723646.1981.10642213

Wu, W. C., Ma, G., & Cox, D. T. (2016). Modeling wave attenuation induced by the vertical density variations of vegetation. *Coastal Engineering*, *112*, 17–27. https://doi.org/10.1016/j.coastaleng.2016.02.004

Table 1. Seagrass parameters input for the model.

Model period	h_v (m)	b_v (cm)	N (shoots m^{-2})	C_D	$\widetilde{C_D}$
January 1-31, 2011	0.2	0.2	50	0.2	3.0
June 1-30, 2011	0.4	0.4	400	0.4	3.0

Table 2. Model runs and vegetation module setup.

Model runs	Period	Seagrass effects on flow	Seagrass effects on waves
W1	January	No	No
W2	January	Yes	No
W3	January	Yes	Yes
S1	June	No	No
S2	June	Yes	No
S3	June	Yes	Yes

Table 3. A summary of statistical metrics for model validation.

Period	Site	Parameter	Statistics		
			Bias	RMSE	Skill
January, 2011	Bare	Water level	0.07 m	0.09 m	0.95
		Hs	-0.02 m	0.05 m	0.68
		Velocity	0.04 m s^{-1}	0.05 m s^{-1}	0.84
		SSC	-3.44 mg L^{-1}	8.69 mg L^{-1}	0.80
	SG	Water level	0.06 m	0.16 m	0.94
		Hs	0.00 m	0.05 m	0.87
		SSC	-4.33 mg L^{-1}	8.13 mg L^{-1}	0.82
June, 2011	Bare	Water level	0.00 m	0.07 m	0.97
		Hs	0.00 m	0.06 m	0.56
		Velocity	0.07 m s^{-1}	0.06 m s^{-1}	0.69
	SG	Water level	0.10 m	0.07 m	0.96
		Hs	-0.01 m	0.04 m	0.67
		Velocity	0.04 m s^{-1}	0.02 m s^{-1}	0.58

Figure Captions

Figure 1. (a) Bathymetry of the model and grid interface between small and large model domains. The boundary between small and large model grids is highlighted by the gray box. S is the small model domain with a resolution of ~70 m while L represents the large model domain with a resolution of 200 m. The subpanel shows the model grid interface in a selected area highlighted by the black dashed trapezoid. WA is the NOAA tide gauge station (Wachapreague, ID: 8631044) used for water level validation (https://tidesandcurrents.noaa.gov). Coordinates of UTM zone 18N are given in km. (b) Aerial image of the study area (South Bay, VCR) and the distribution of seagrass meadow. The image is from the Virginia Institute of Marine Science Submerged Aquatic Vegetation (SAV) program (http://web.vims.edu/bio/sav). Orange triangles show the unvegetated site (Bare) and the seagrass site (SG) used for model validation. Red dashed lines show the transect location for water and sediment flux monitoring. (c) Directional distribution of winds in the study area in January and June, 2011. The wind data is from the NOAA National Data Buoy Center (Station CHLV2; https://www.ndbc.noaa.gov/station_page.php?station=chlv2). For the full record of model forcing during each time period, please refer to Figure S1.

Figure 2. Comparison of measured and modeled hydrodynamic and suspended sediment conditions during a 4-day period at the bare site (Bare): (a) water level, (b) Hs, (e) velocity, and (f) SSC in January, 2011, and (c) water level, (d) Hs, (g) velocity, and (h) SSC in June, 2011. Black lines represent observational data, and red dots (lines) show model simulation results.

Figure 3. Comparison of measured and modeled hydrodynamic and suspended sediment conditions during a 4-day period at the seagrass site (SG): (a) water level, (b) Hs, and (e) SSC in January, 2011, and (c) water level, (d) Hs, (f) depth-averaged velocity, and (g) SSC in June, 2011. Black lines represent observational data, and red dots (lines) show model simulation results.

Figure 4. Box plots of modeled (a) depth averaged velocity, (b) Hs, and (c) total SSC at the bare site and seagrass site output from model runs W3 (January 1-31) and S3 (June 1-30) that include seagrass effects on flow and waves.

Figure 5. (a) Distribution of depth averaged velocity at peak ebb conditions from model run S3 (with effects of summer seagrass densities on flow and waves). The color scale indicates the magnitude of velocity, while arrows show flow direction. (b) Wave height difference between model runs S2 (without seagrass wave attenuation effects) and S3 (with seagrass wave attenuation effects) during a strong wind wave event (June 17). The red dashed line shows the meadow outline.

Figure 6. (a) Cumulative water flux and (b) cumulative sediment flux into/out of seagrass meadows through model monitoring transects during each simulation period (January 1-31 and June 1-30, 2011). Model runs W1 and S1 are without seagrass effects in winter and summer, respectively, while W3 and S3 include seagrass effects on reduction in flow and waves. Positive values denote water/sediment input while negative values indicate export of water/sediment from the meadow.

Figure 7. Total SSC distribution output from: (a) model run S1 (without seagrass effects) during a storm on June 17 and (b) model run S3 (with seagrass effects on flow and waves) during the same period. The red dashed line shows the meadow outline.

Figure 8. Velocity (a) and bed shear stress (b) change as a function of seagrass density at the seagrass site. The velocity and bed shear stress are normalized with respect to model run results without seagrass effects. Seagrass parameters used in these flow simulations are: h_v= 0.4 m, b_v = 0.4 cm, and C_D = 0.4.

Figure 9. (a) Velocity difference at the western edge of seagrass meadow during peak ebb between model runs S1 (the reference summer simulation without seagrass effects) and S3 (with seagrass effects on flow and waves). Arrows show the flow direction and magnitude in S3. The color scale indicates velocity changes relative to the flow speed in model run S1 (Figure 5a). Positive values denote velocity acceleration while negative values denote velocity reduction. The red dashed line shows the meadow outline. (b) Water flux along the cross-meadow transect during the same time period. The transect location is shown in black dashed line in (a).

Figure 10. Density distributions of bed shear stress at the seagrass site in January (a) and June (b). Dashed lines denote mean shear stress of each model run. Model runs W1 and S1 are without seagrass effects; W2 and S2 include seagrass effects on flow; and W3 and S3 include seagrass effects on attenuation of flow and waves.

Figure 11. Spatial erosion/deposition patterns from simulations: (a) W3, (b) S3. Both simulations are run with seagrass effects on flow and waves for the entire month.

Figure 12. Relationship between deposition within seagrass meadows and the distance to meadow edge. Deposition data were extracted from six transects (black lines in the lower bottom map) in model run S3. The equation of the fitting curve is $log_{10}Y = -0.002X - 2.165$, with $R^2 = 0.99$.

Figure 13. Net sediment flux into/out of seagrass meadows as a function of winter seagrass density. Positive values denote net sediment input while negative values indicate net sediment export.

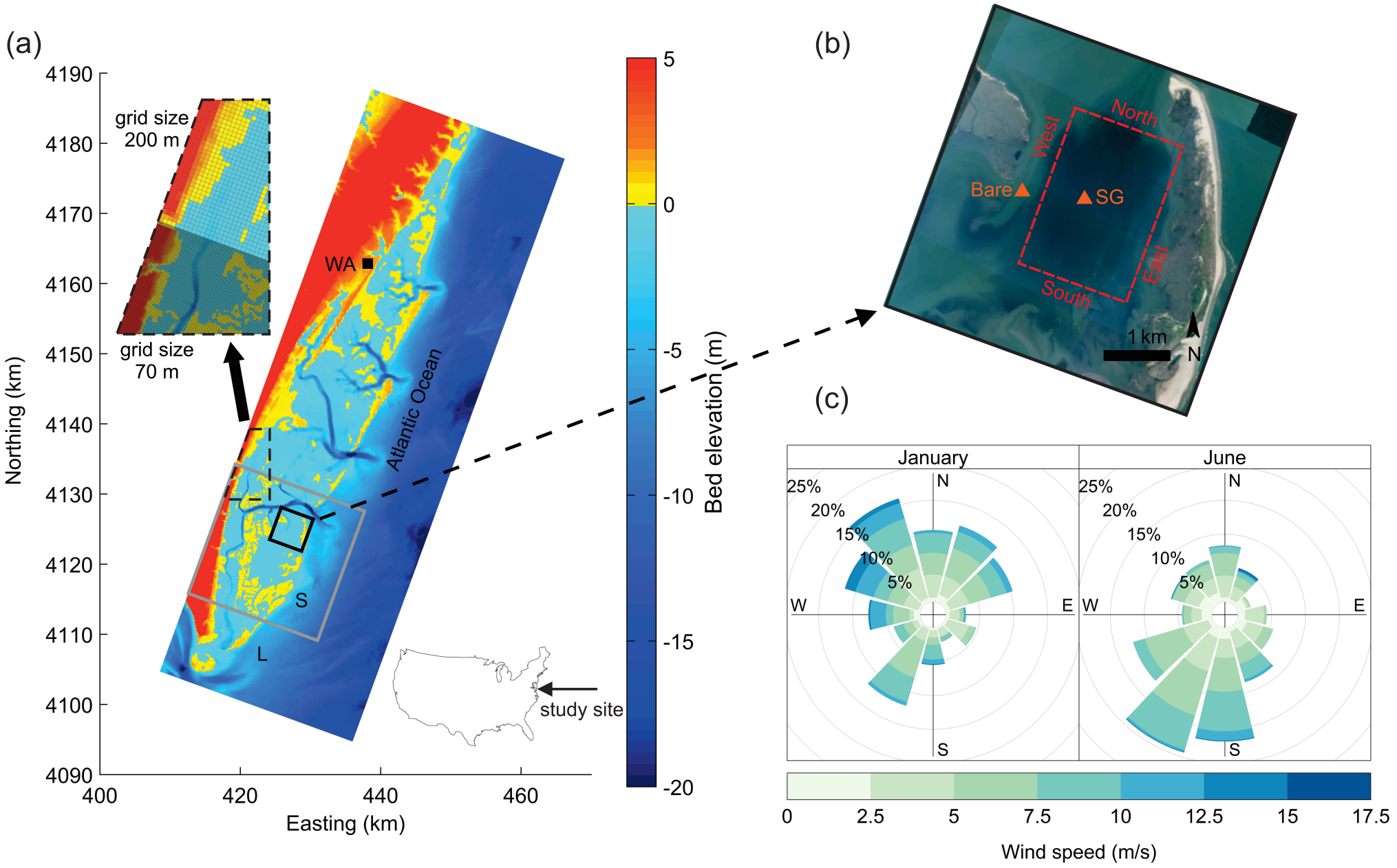
(a)
grid size
200 m
grid size
70 m
WA
Atlantic Ocean
S
L
study site
Northing (km)
Easting (km)
Bed elevation (m)
4190
4180
4170
4160
4150
4140
4130
4120
4110
4100
4090
400
420
440
460
5
0
-5
-10
-15
-20
(b)
North
West
East
South
Bare
SG
1 km
N
(c)
January
June
N
S
W
E
25%
20%
15%
10%
5%
0
2.5
5
7.5
10
12.5
15
17.5
Wind speed (m/s)

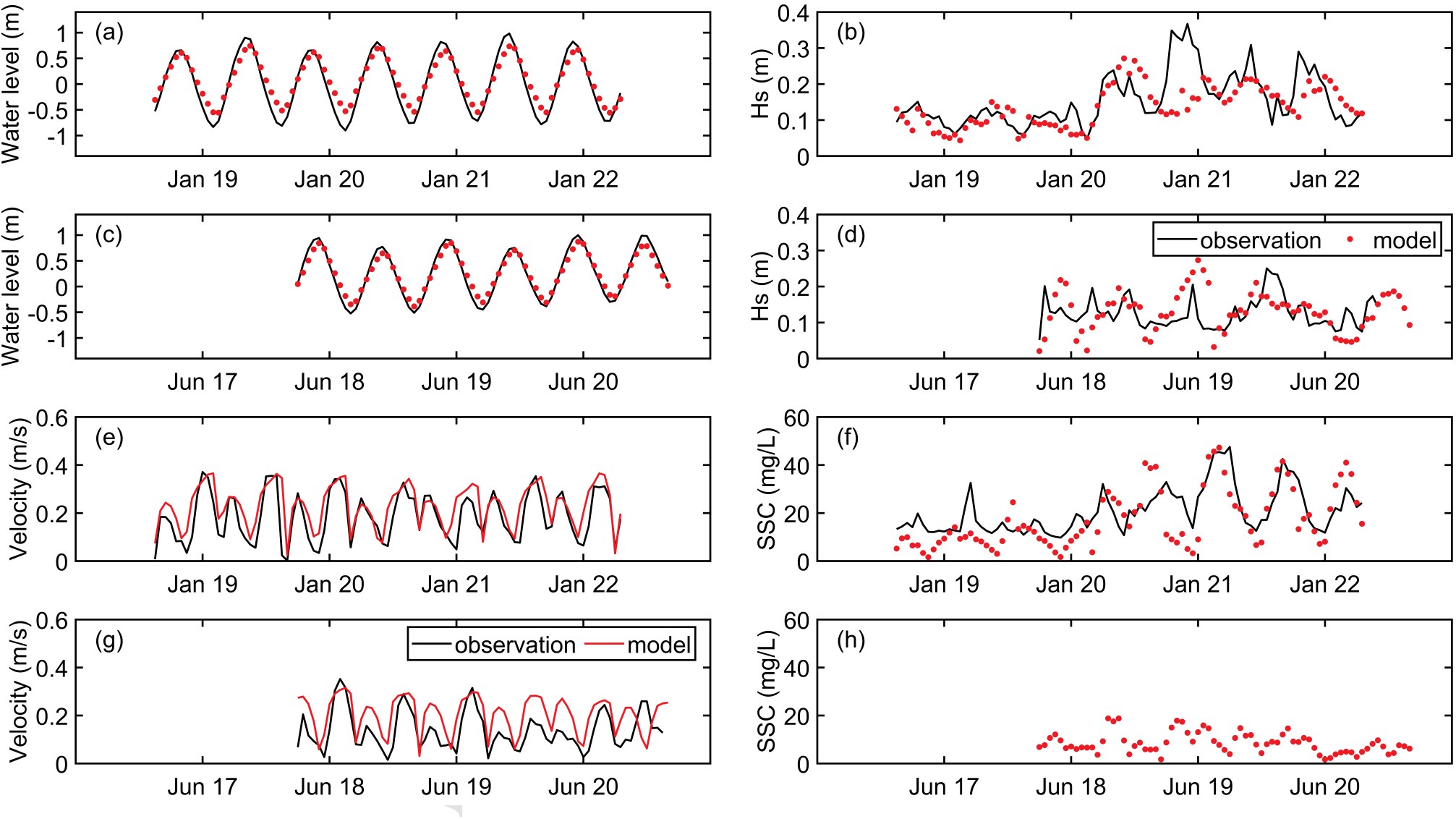

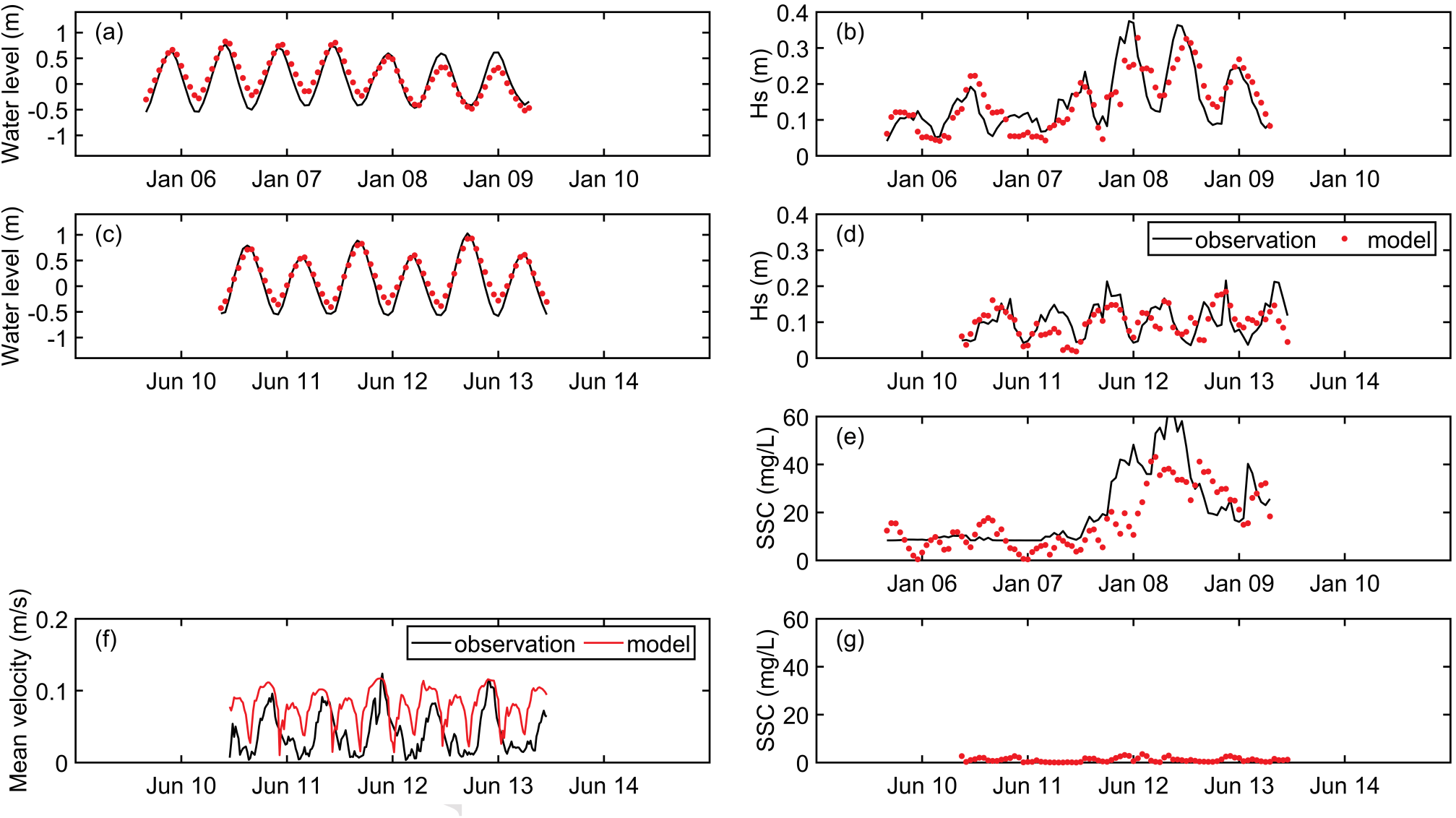

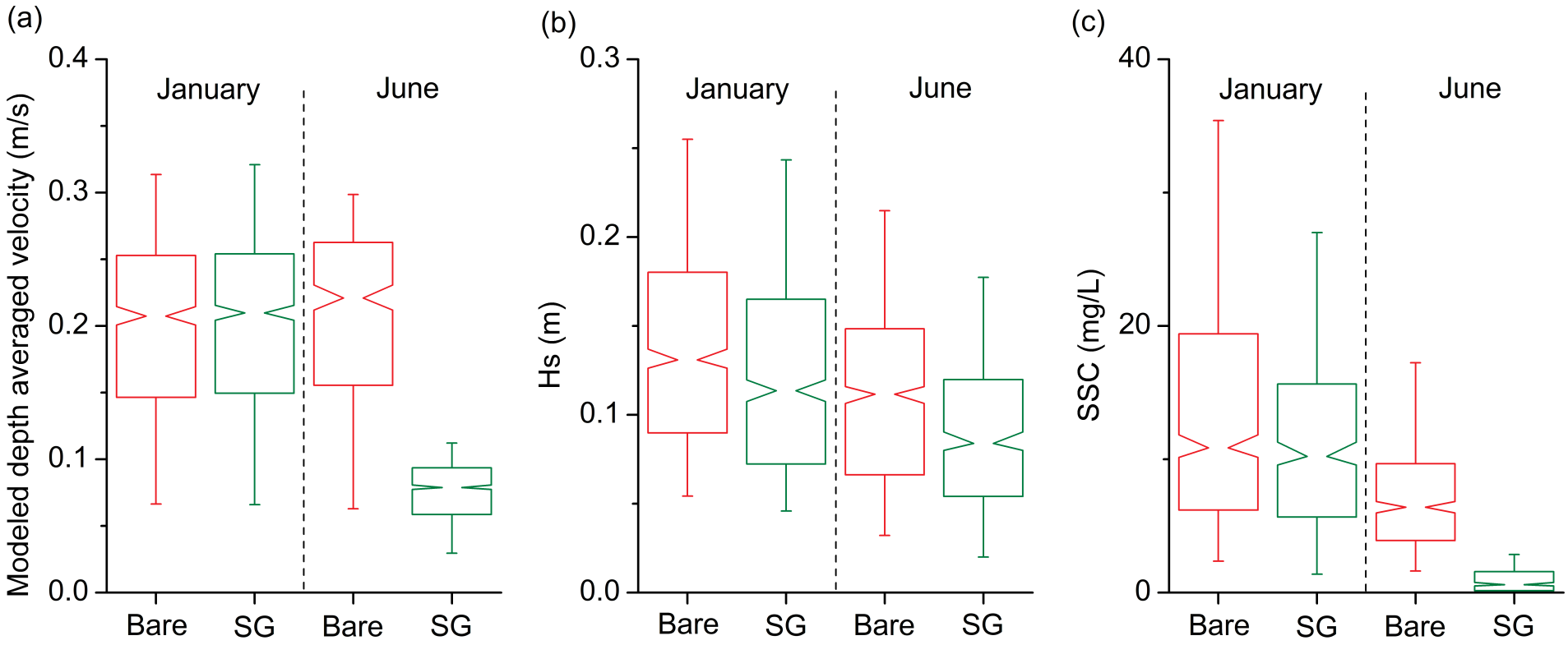
(a)
Modeled depth averaged velocity (m/s)
0.4
0.3
0.2
0.1
0.0
January
June
Bare
SG
Bare
SG
(b)
Hs (m)
0.3
0.2
0.1
0.0
January
June
Bare
SG
Bare
SG
(c)
SSC (mg/L)
40
20
0
January
June
Bare
SG
Bare
SG

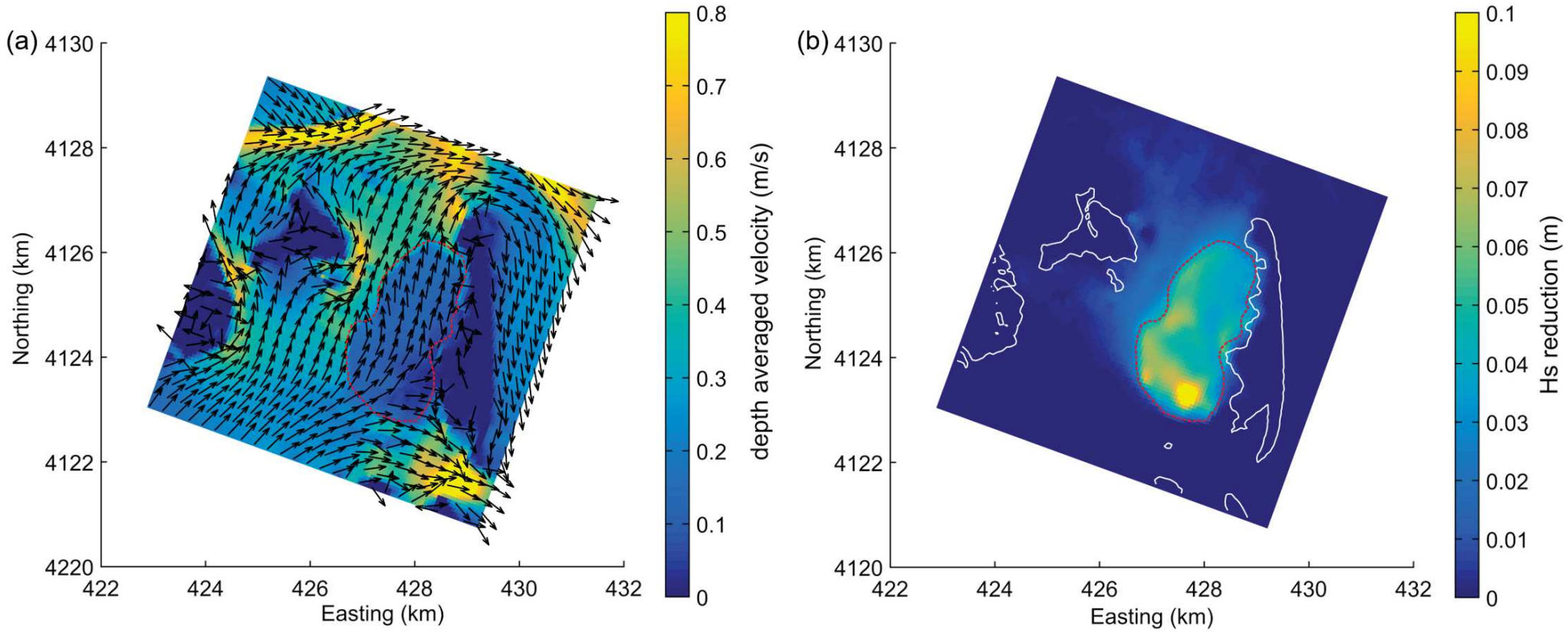
(a)
(b)
Northing (km)
Easting (km)
depth averaged velocity (m/s)
Hs reduction (m)
4130
4128
4126
4124
4122
4220
4120
422
424
426
428
430
432
0.8
0.7
0.6
0.5
0.4
0.3
0.2
0.1
0
0.09
0.08
0.07
0.06
0.05
0.04
0.03
0.02
0.01

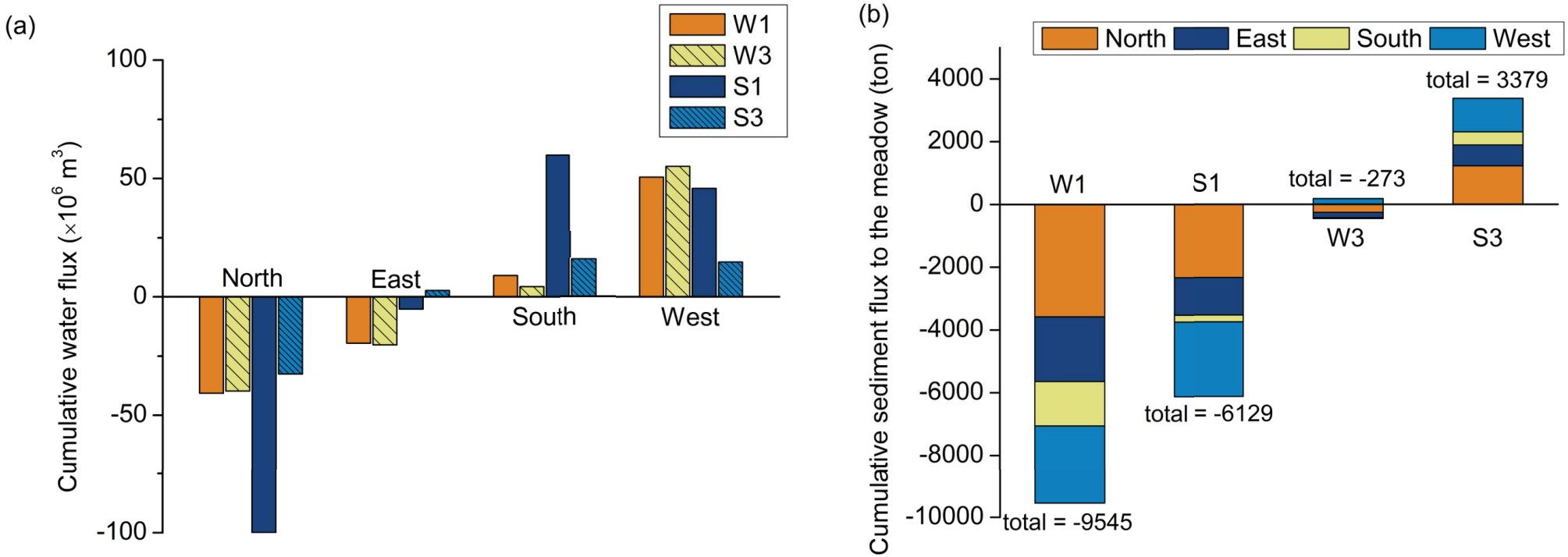
(a)
W1
W3
S1
S3
100
50
0
-50
-100
Cumulative water flux (×10^6 m^3)
North
East
South
West
(b)
North
East
South
West
4000
2000
0
-2000
-4000
-6000
-8000
-10000
Cumulative sediment flux to the meadow (ton)
W1
S1
total = -273
total = 3379
W3
S3
total = -6129
total = -9545

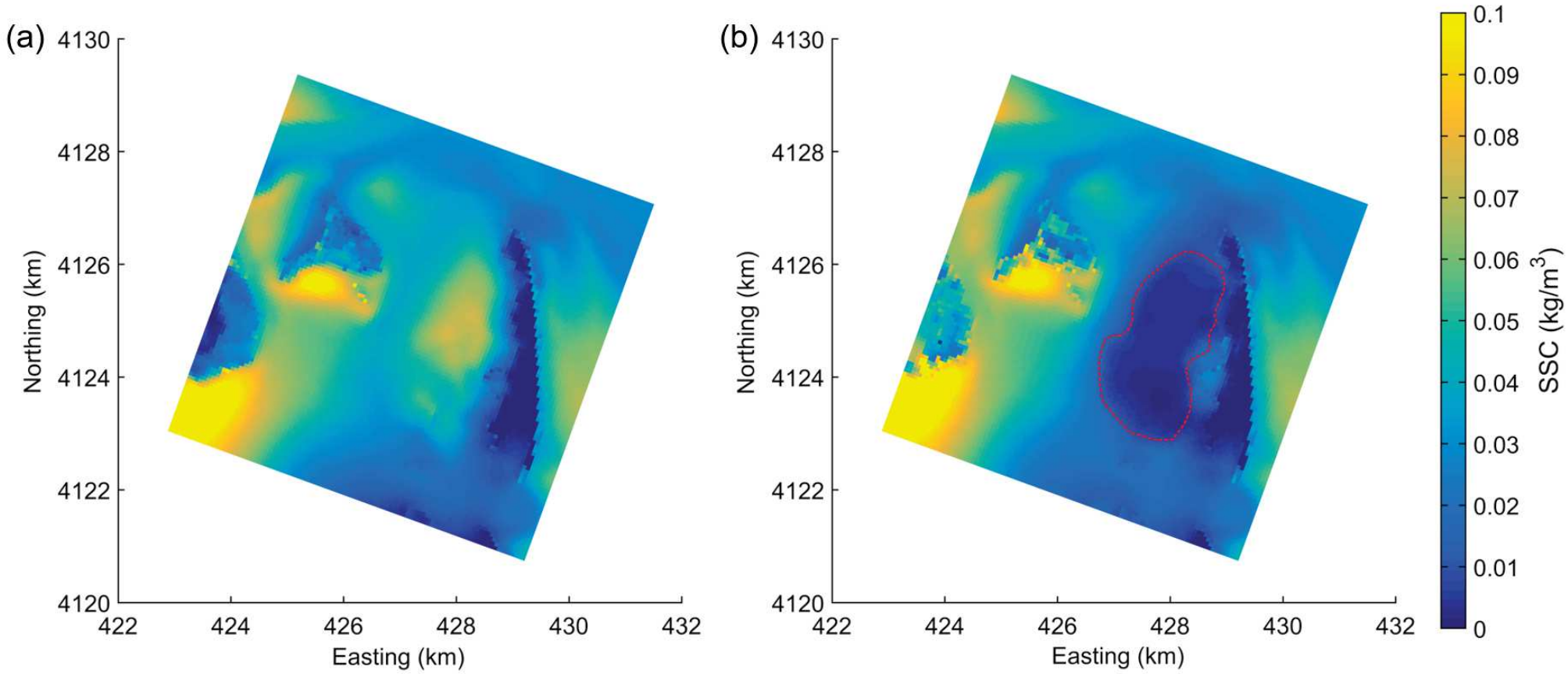
(a)
(b)
Northing (km)
Easting (km)
4120
4122
4124
4126
4128
4130
422
424
426
428
430
432
SSC (kg/m^3)
0
0.01
0.02
0.03
0.04
0.05
0.06
0.07
0.08
0.09
0.1

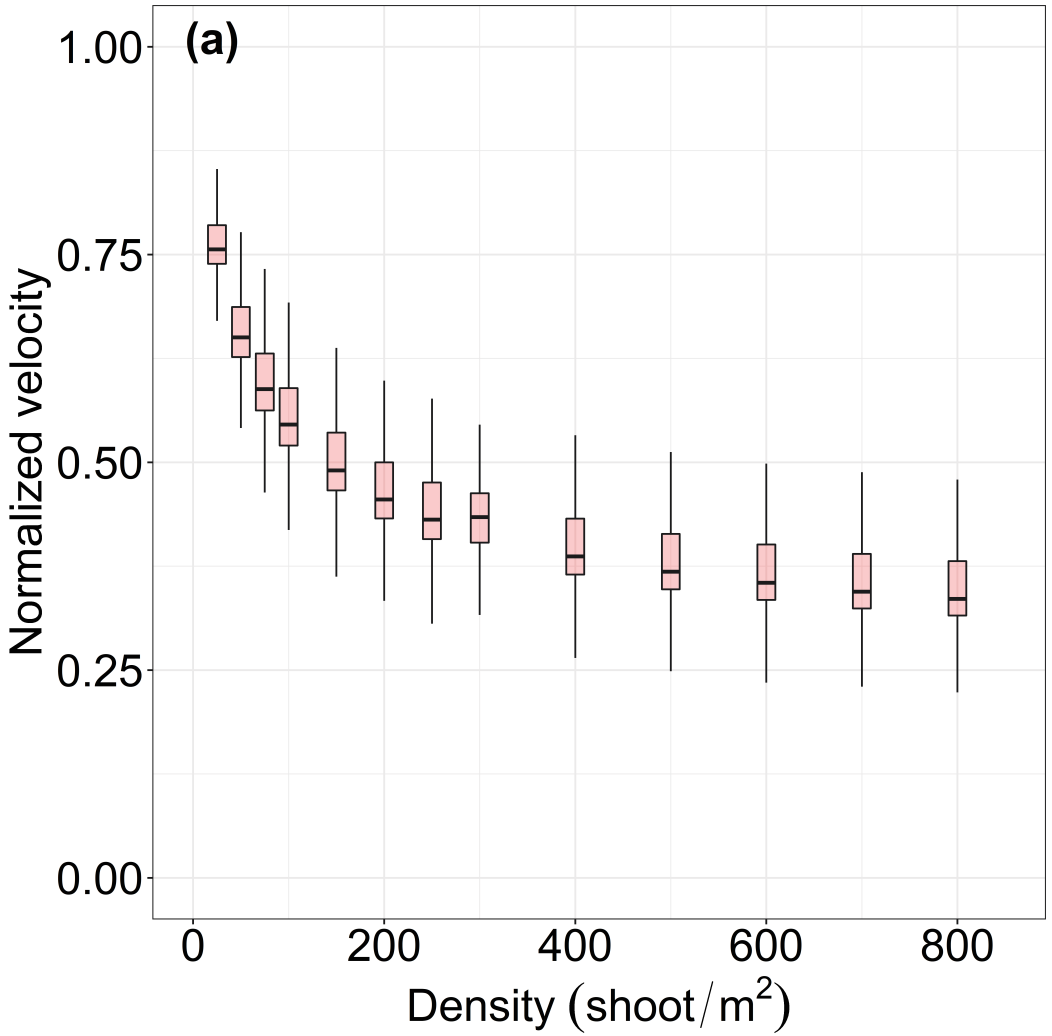
(a)
1.00
0.75
0.50
0.25
0.00
Normalized velocity
0
200
400
600
800
Density (shoot/m^2)

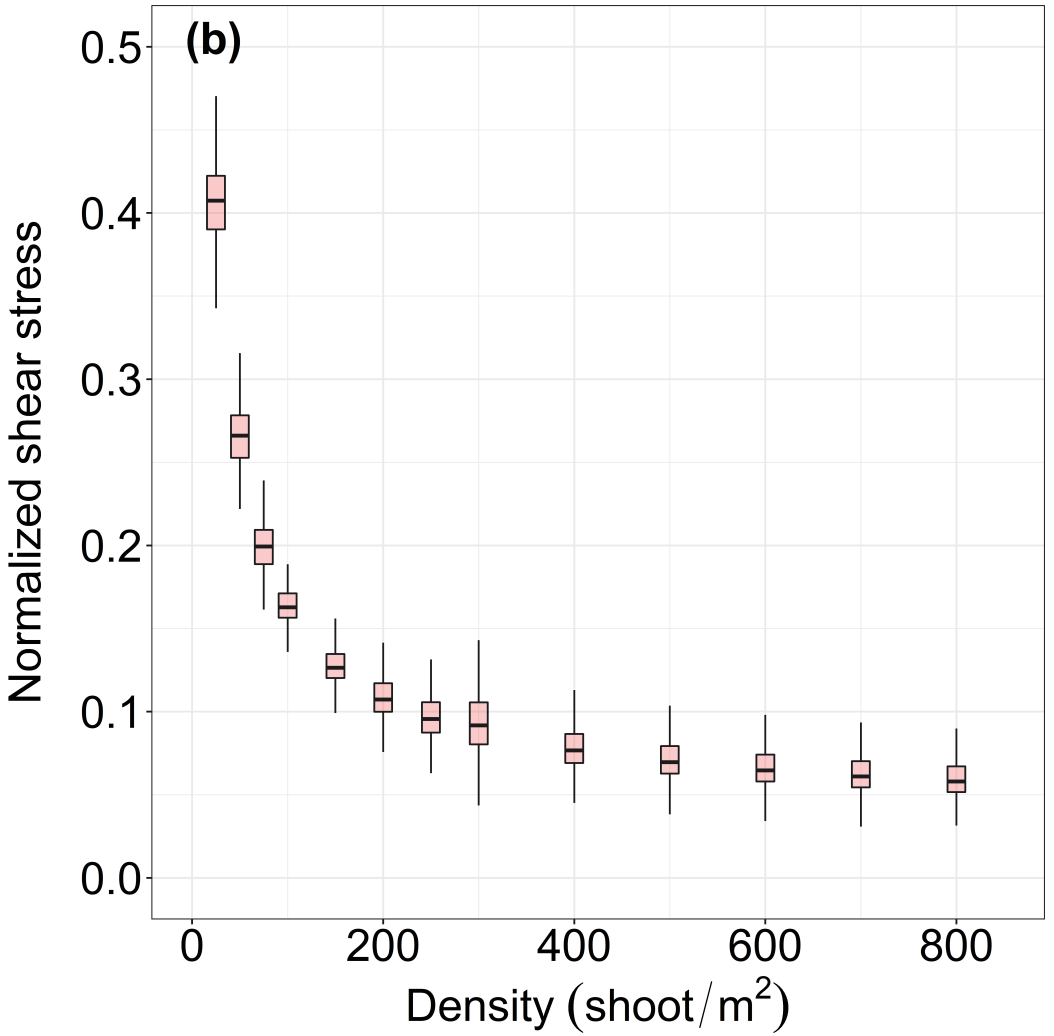
(b)
0.5
0.4
0.3
0.2
0.1
0.0
Normalized shear stress
0
200
400
600
800
Density (shoot/m^2)

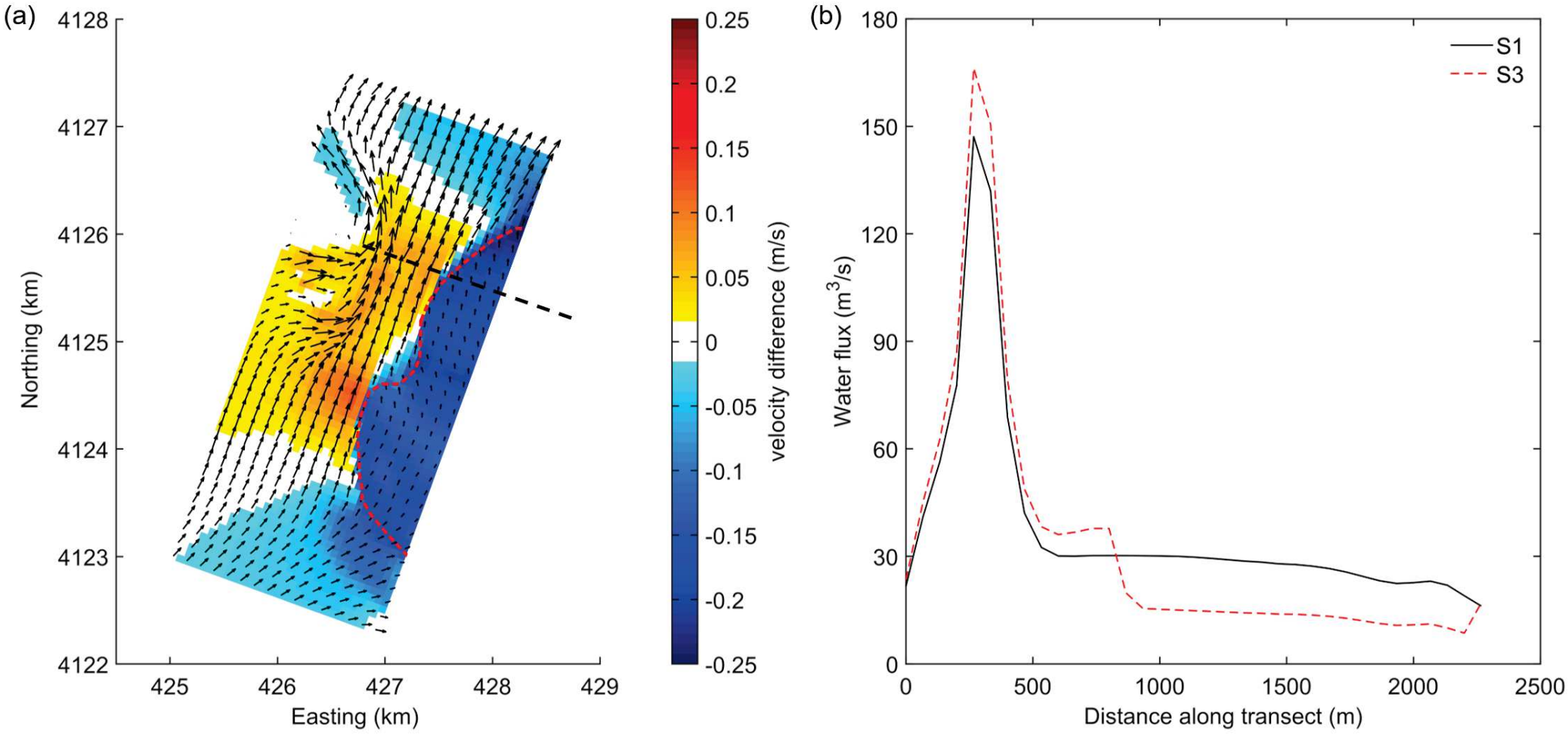
(a)
4128
4127
4126
4125
4124
4123
4122
Northing (km)
425
426
427
428
429
Easting (km)
0.25
0.2
0.15
0.1
0.05
0
-0.05
-0.1
-0.15
-0.2
-0.25
velocity difference (m/s)
(b)
180
150
120
90
60
30
0
Water flux (m3/s)
S1
S3
0
500
1000
1500
2000
2500
Distance along transect (m)

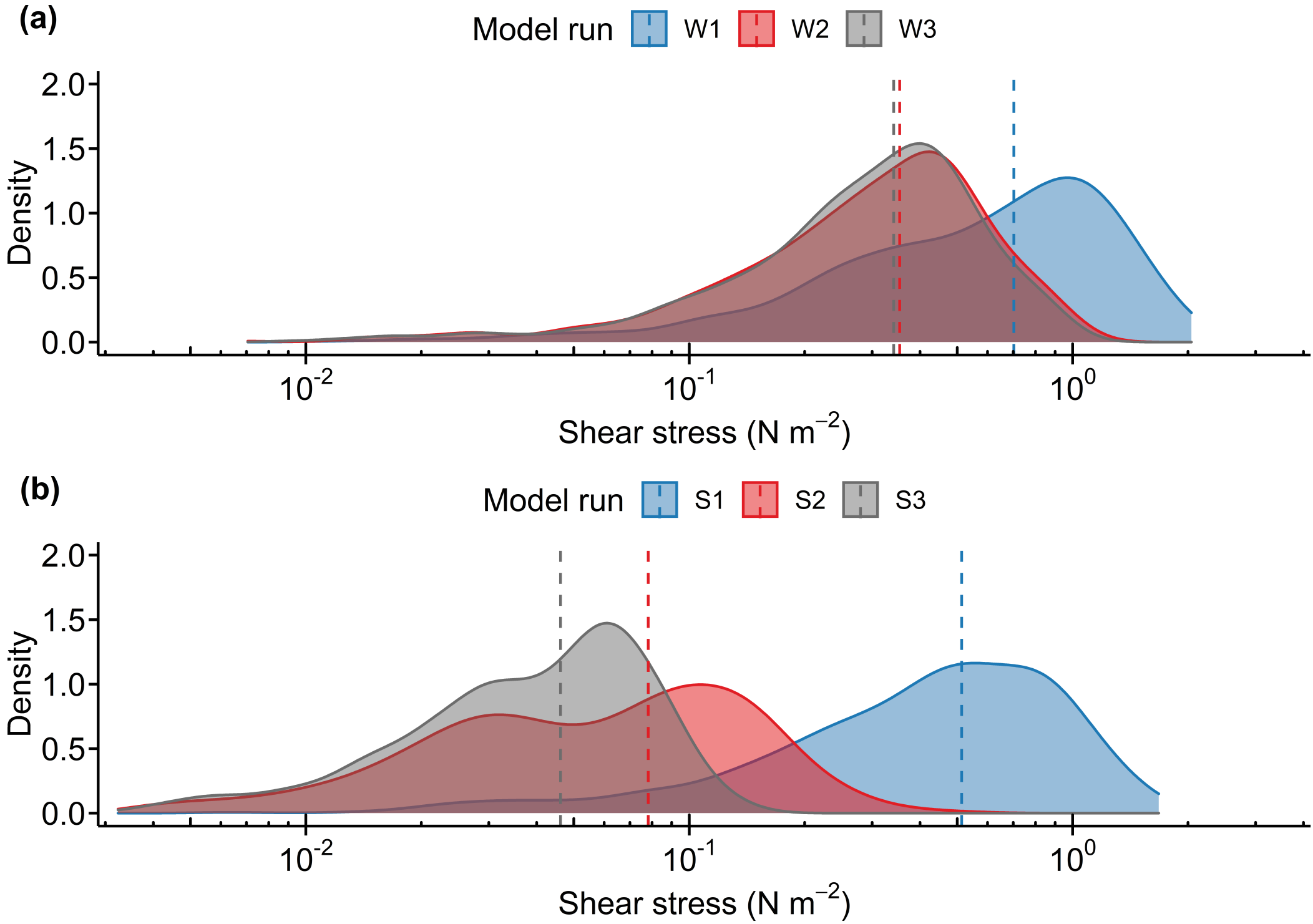
(a)
Model run
W1
W2
W3
Density
2.0
1.5
1.0
0.5
0.0
10^{-2}
10^{-1}
10^{0}
Shear stress (N m^{-2})
(b)
Model run
S1
S2
S3
Density
2.0
1.5
1.0
0.5
0.0
10^{-2}
10^{-1}
10^{0}
Shear stress (N m^{-2})

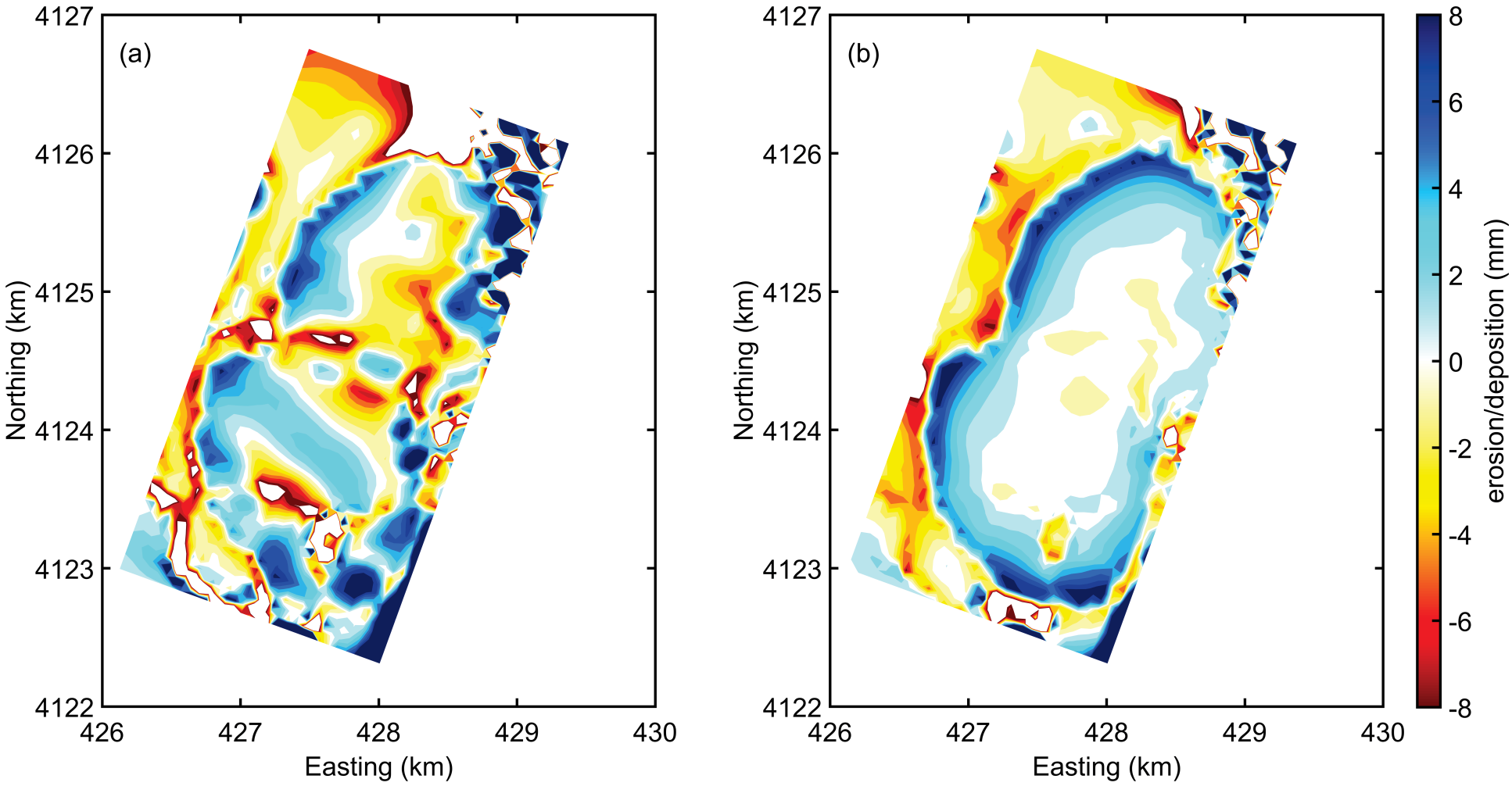
(a)
(b)
Northing (km)
Easting (km)
4127
4126
4125
4124
4123
4122
426
427
428
429
430
8
6
4
2
0
-2
-4
-6
-8
erosion/deposition (mm)

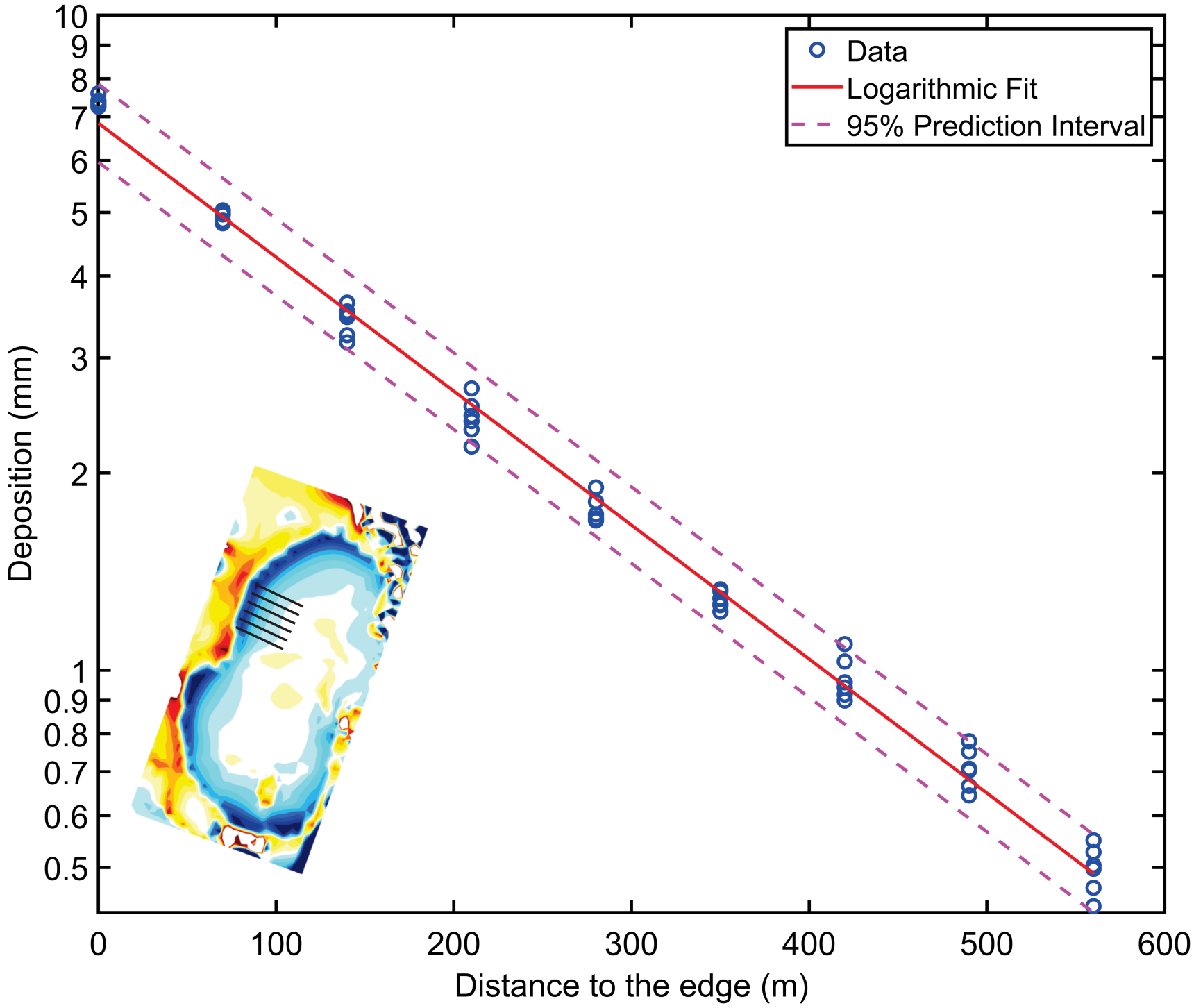
Data
Logarithmic Fit
95% Prediction Interval
Deposition (mm)
Distance to the edge (m)
10
9
8
7
6
5
4
3
2
1
0.9
0.8
0.7
0.6
0.5
0
100
200
300
400
500
600

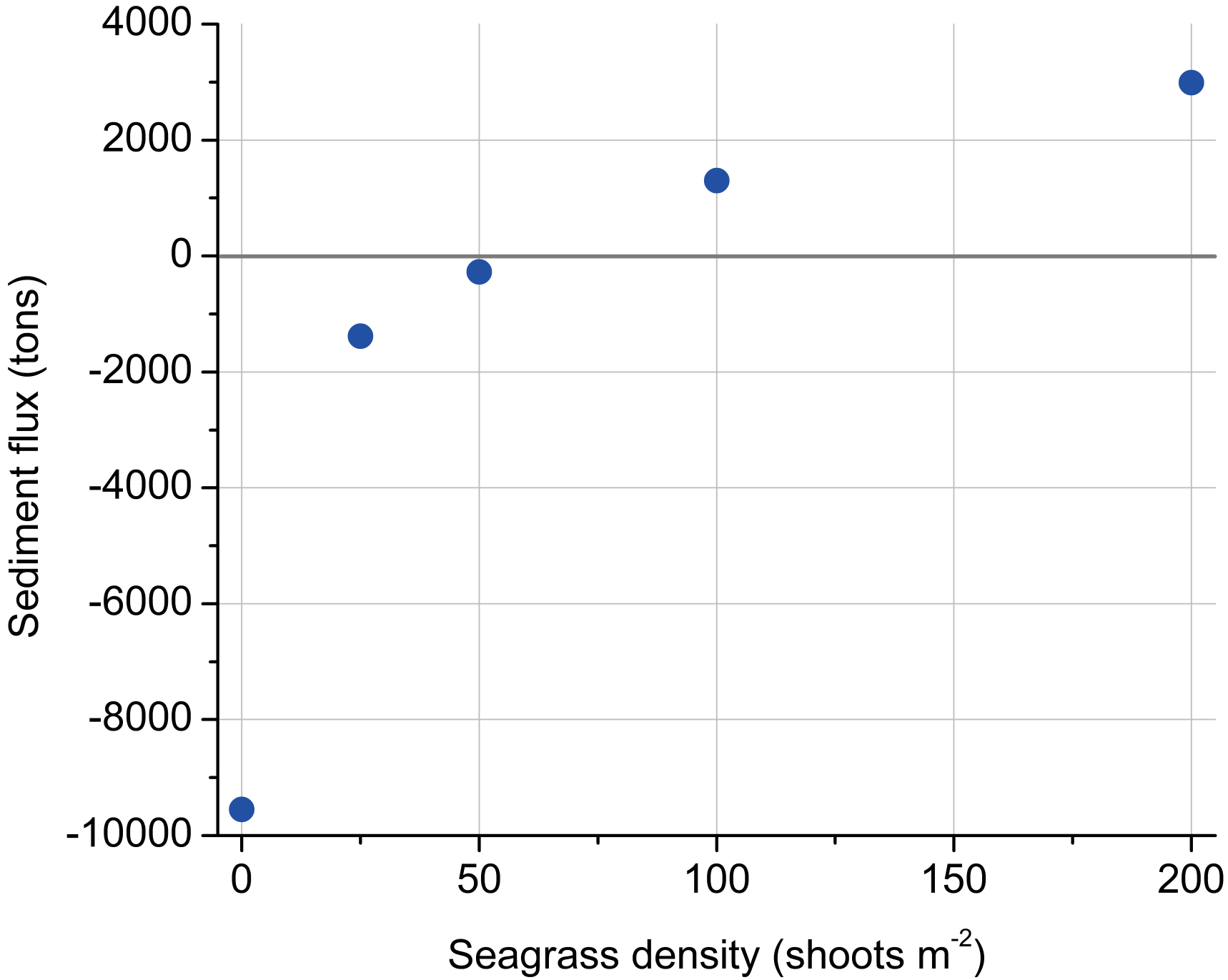
4000
2000
0
-2000
-4000
-6000
-8000
-10000
Sediment flux (tons)
0
50
100
150
200
Seagrass density (shoots m-2)